TAMPEREEN TEKNILLINEN YLIOPISTO
TAMPERE UNIVERSITY OF TECHNOLOGY

NIRAJAN OJHA

BOROSILICATE GLASS WITH ENHANCED HOT FORMING PROPERTIES AND CONVERSION TO HYDROXYAPATITE

Master of Science thesis

Examiner: Dr. Jonathan Massera (Docent, Assistant Professor, Academy research fellow)
Examiner and topic approved by the Faculty Council of the Faculty of Natural Science
on 3rd February 2016

ABSTRACT

NIRAJAN OJHA: Borosilicate glass with enhanced hot forming properties and conversion to hydroxyapatite
Tampere University of technology
Master of Science Thesis, 60 pages,
June 2016
Master's Degree Programme in Biomedical Engineering
Major: Biomaterials
Examiner: Dr. Jonathan Massera (Academy research fellow)

Keywords: Bioactive glass, DTA, FTIR, pH, SBF, scaffold, sintering, TRIS

Bioactive glasses are capable of reacting with physiological fluids to form a hydroxyapatite (HA) layers. This layer, with similar composition than the mineral part of the bone, leads to firm bond between the glass and the tissue. Silicate based bioactive glasses commonly convert slowly and incompletely to HA due to their non-congruent dissolution. It was found in previous clinical studied that typical bioactive glass remains at the surgical site even 14 years' post-surgery.

The dissolution and reaction mechanism, leading to the precipitation of a HA layer is mainly due to the bioactive glass loose structure. However, such loose structure also inhibits any hot forming of the glass. Indeed, sintering of commercial bioactive glasses led to scaffolds with very low mechanical properties and partially to fully crystallized scaffolds. The surface crystallization of these glasses decreased their bioactivity.

This thesis uses the glass S53P4 as a reference as it is well studied and commercially available. As for all commercially available silicate bioactive glasses, glass S53P4 cannot be hot formed without crystallization and does not convert fully into HA. Thus, glasses with partial to almost full substitution of the SiO_2 with B_2O_3 were developed. The aim is to define new glass composition that have thermal and structural properties allowing for heat sintering while converting faster to HA. In general, the addition of boron within the silicate glass led to a material more prone to dissolve in aqueous solution. The reaction of the glass and its conversion into hydroxyapatite was also faster. The glass labelled B25, B50 and B75 were found to be the most suited to be sintered into porous scaffolds.

Scaffold were processed using three particles size (<250 µm, 250 – 500 µm and >500µm). The porosity was found to decrease with decreasing the particles size (at similar sintering temperature) and increasing the sintering temperature (at constant particle size). All the scaffolds produced were found to be amorphous. Scaffolds (particle size 250 – 500µm) with 50% overall porosity were immersed in SBF for up to 168h. The compression strength decreased with increasing the immersion time. All the scaffold maintained their ability to precipitate a HA layer at their surface. The newly developed glasses were found to be suitable for future, more sophisticated scaffold manufacturing for tissue engineering.

PREFACE

I would like to take this opportunity to show my appreciation to each and every person who has contributed to this successful thesis work. This Master of Science thesis has been completed at the laboratory of Biomaterials and Tissue Engineering at Tampere University of Technology. The thesis work was quite inspiring and strenuous but it provided me thorough understanding of bioactive glasses and their properties. I am very happy to have had the chance to work as a research assistant within the department and complete my thesis work.

Firstly, and most importantly I would like to mention the role of Dr. Jonathan Massera for believing in me and providing an opportunity to undertake this thesis topic. He has always been a cheerful and inspiring supervisor. He has always trusted me in my work and had been flexible too during my working hours. His guiding and supervision during the thesis was immense and he was helpful in making me understand new concepts which were unfamiliar to me. To be a part of his research was an honor for me and I would definitely like to work with him in the future.

Finally, I also would like to thank my parents for support and blessings, my wife Srijana Ghimire for her encouragement, my daughter Shravya Ojha for her cheerful smile after a long day of work and all my friends.

Tampere, 10.06.2016

Nirajan Ojha

CONTENTS

LIST OF FIGURES

LIST OF TABLES

LIST OF SYMBOLS AND ABBREVIATIONS

3D	Three Dimension
ACP	Amorphous calcium phosphate
A.U.	Arbitrary unit
BO	Bridging Oxygen
CaP	Calcium Phosphate
DTA	Differential thermal analysis
FTIR	Fourier Transformed Infra-Red Spectroscopy
g	Gram
HA	Hydroxyapatite
M	Molecular Mass
mol	Mole
mol%	mole percentage
NBO	Non bridging Oxygen
SA	Surface Area
SA/V	Surface area to volume ratio
SBF	Simulated Body Fluid
TRIS	tris(hydroxymethyl)aminomethane
T_g	Glass transition temperature
T_L	Liquidus temperature
T_p	Crystallization peak temperature
T_x	Temperature at onset of crystalization
V_m	Molar Volume
wt%	Weight percentage
XRD	X-ray diffraction
µCT	micro computed tomography
ρ	density

1. INTRODUCTION

With the advancement in the medical science and engineering, there has always been an interest to ease medical complication by developing new methods and materials. For the sake of betterment of mankind various materials are being researched and innovated for use in humans. One of the biggest field in this innovation is biomaterials. According to Williams "A biomaterial is a substance that has been engineered to take a form which, alone or as part of a complex system, is used to direct, by control of interactions with components of living systems, the course of any therapeutic or diagnostic procedure, in human or veterinary medicine" (Williams 2009). Biomaterial is a broad subject and has been classified by various authors and administrations differently. In regards to the tissue reaction, biomaterials can be: biotolerant (separated from the bone tissue by fibrous tissue), bioactive (that have property to form chemical bond with bone tissue) or bioinert (no chemical reaction occur between implant and the tissue) (Bergmann 2013). This thesis focuses mainly on bioactive materials.

A bioactive material is able to elicit a specific biological response at the interface of the material that results in the formation of a bond between the tissues and the material (Hench *et al.* 1972). Bioactive glasses are a subset of inorganic bioactive materials. They are capable of reacting with physiological fluids to form firm bonds to bone through the formation of hydroxyapatite layers, a main constituent of bone, and the biological interaction of collagen with the material surface (Hench, 1998). Bioactive glasses are osteoconductive, i.e., that they have the ability to grow new bones at their surface. They not only form a bond with hard but also with soft tissues. 45S5 (Bioglass®) and S53P4 (BonAlive®) are the most studied bioactive glass for biomedical applications. Both these glasses are FDA approved.

The most studied bioactive glasses are silicate-, phosphate- and borate-based. Silicate based bioactive glass are the most commercially used bioactive glasses. They are used mainly as granules and coating in bone regeneration, dental, wound healing and maxillofacial applications. Borate glasses have shown promising results in bone regeneration and angiogenesis (Bi *et al.* 2013) and phosphate glass have been found as alternative to silicate glass in bone repair and reconstruction (Clement *et al.* 1999). The main difference between these glasses being is the way in which they dissolve and react *in vitro* and *in vivo*. Silicate glasses are known to dissolve in a non-congruent manner, i.e. alkaline and alkaline earth present in the glass are released at a higher rate than the Si ions that results in the formation of a thick Si-rich layer onto which the hydroxyapatite will precipitate (Hench 1998). At the contrary, phosphate and borate bioactive glasses de-

grades in a congruent manner, i.e. that all ions are released at the same rate and the base glass composition does not change with respect to the immersion time (Bunker *et al.* 1984, Massera *et al.* 2014a, Yao *et al.* 2007)). Often, this leads to a more control and a more complete dissolution.

There has been an increasing interest in porous glasses for applications where bone ingrowth is needed. Especially, there is a clinical demand for artificial bone graft materials or bioactive scaffolds that can stimulate bone regeneration by acting as temporary templates for vascularized bone growth (Amini *et al.* 2012). The scaffold should have an interconnected pore structure, with interconnected pore sizes that are greater than 100 μm (Jones *et al.* 2003) but subsequent studies have shown better osteogenesis for implants with pores >300 μm (Tsuruga *et al.* 1997). Relatively larger pores favor direct osteogenesis, since they allow vascularization and high oxygenation. However, increase in porosity leads to poor mechanical properties. The compression strength of porous glassy implants has been achieved in the same order as that of cancellous bone (Jones *et al.* 2006). The compressive strength of cancellous bone is 2-12 MPa and that of cortical bone 100-230 MPa (Heikkilä 2011). To reach higher mechanical properties a higher sintering temperature is usually used. However, it was found that the high thermal treatment increases the strength, but also induced crystallization and reduces the porosity (Fagerlund 2012). There have been studies on the effectiveness of the porous scaffold made form silicate bioactive glass (Jones *et al.* 2006) and composites of phosphate-based bioactive glasses with PLA (Georgiou *et al.* 2007). However, in most case it was found that in order to reach proper sintering, the temperature to process the scaffolds was in the glass crystallization domain. Commercial silicate bioactive glass S53P4 and 45S5 are prone to crystallization at temperature at which it should be hot formed, inhibiting proper particles sintering prior to crystallization (Massera *et al.* 2012). Crystallization was not only found to limit effective particle sintering but to also reduce the glass' bioactivity (Fagerlund *et al.* 2012a).

Recent work has shown the ability to control the degradation rate of bioactive glass by manipulating its composition. For example, by partially replacing the SiO_2 in silicate 45S5 with B_2O_3 (yielding a borosilicate bioactive glass), or fully replacing the SiO_2 with B_2O_3 (producing a borate bioactive glass), the degradation rate can be varied over a wide range (Huang *et al.* 2006). Silicate based bioactive glasses commonly convert slowly and incompletely to HA, resulting in the long-term presence of unconverted glass *in vivo* but borate bioactive glass has been found to degrade faster and convert more completely to HA (Rahaman *et al.* 2014). By controlling the glass composition, it should be possible to match the degradation rate of borate-based bioactive glass with the bone regeneration rate (Rahaman *et al.* 2011, Greenspan 1999). The bioactivity of the glass which is measured by the rate at which it converts to HA, can be varied from hours to months, depending on the composition of the glass (Huang *et al.* 2006). Borate bioactive glasses have shown to support cell proliferation and differentiation *in vitro* as

well as tissue infiltration *in vivo* (Rahaman *et al.* 2011). Understanding the *in vitro* properties of the glass in SBF and TRIS buffer leads to somewhat approximation of the glass behaviors *in vivo*.

This thesis consists of a theoretical background presented in chapter 2. This chapter gives the key concepts that are relevant to the thesis. Chapter 3 describes the experimental and key methods applied in the thesis. The main results are discussed in Chapter 4. Conclusion of the thesis is presented in chapter 5 and reports the key findings.

2. THEORETICAL BACKGROUND

2.1 Bioactive glass

Bioactive glasses are osteoconductive and osteoinductive materials as it supports new bone growth along the bone–implant interface as well as within the implant away from the bone–implant interface (Rahaman *et al.* 2011). The glass, when used as implants, is generally believed to dissolve completely and help in bone growth, however this does not always hold true for all glass compositions and there have been evidence of glass remnants even years after implantation (Peltola *et al.* 2011). The first bioactive glasses were within the Na_2O-CaO-P_2O_5-SiO_2 oxide-system, and later, K_2O, MgO and/or B_2O_3 were added to improve the hot-working properties of the glasses (Hench 1996, Brink 1997). Other elements, such as Ag, Al, Cu, Sr, and Zn, have also been included either directly to the glass structure or in coatings on glass to further enhance the antibacterial properties and cell response of the glass (Rahaman *et al.* 2011, Andersson *et al.* 1990, Blaker *et al.* 2004). Bioactive glasses are used in different forms and size such as monoliths, particulates and coatings (Figure 1). The most studied bioactive glasses are silicate, borate and phosphate-based. Since, this thesis is focused mainly on silicate and borate glass, a short review of these glasses is given below.

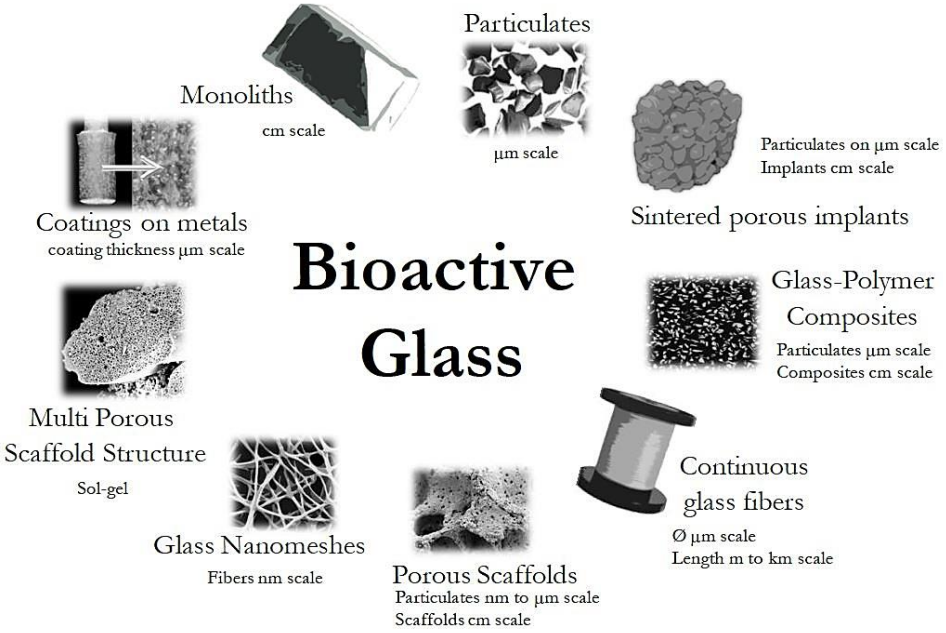

Figure 1: *Various product forms manufactured from bioactive glasses with various methods (Fagerlund, 2012)*

2.1.1 Silicate bioactive Glass

The bioactive glass 45S5 developed by (Hench *et al.* 1972) and S53P4 glass developed by (Andersson *et al.* 1990) are the most clinically used silicate bioactive glasses. They are commercially available as Bioglass® and Bonalive® respectively. Their composition, in wt%, is given in Table 1.

Table 1: *Composition of Commercially available Silicate bioactive glass*

Glass	SiO_2	Na_2O	CaO	P_2O_5
45S5	45	24.5	24.5	6
S53P4	53	23	20	4

There are five stages governing the reaction of silicate bioactive glasses when in contact with a physiological medium (Hench, 1991).

1. Rapid ion exchange reactions between the glass network modifiers (Na^+ and $Ca^{2+)}$ with H^+ (or H_3O^+) ions from the solution, leads to hydrolysis of the silica groups and the creation of silanol (Si–OH) groups on the glass surface. The pH of the solution increases due to the consumption of H^+ ions.
2. The increase in pH (or OH^- concentration) leads to attack of the SiO_2 glass network, and the dissolution of silica, in the form of silicic acid, $Si(OH)_4$, into the solution, and the continued formation of Si–OH groups on the glass surface.
3. Condensation and polymerization of an amorphous SiO_2^- rich layer on the surface of the glass depleted in Na^+ and Ca^{2+}.
4. Further dissolution of the glass, coupled with migration of Ca^{2+} and $(PO_4)_3$ ions from the glass through the SiO_2-rich layer and from the solution, leading to the formation of an amorphous calcium phosphate (ACP) layer on the surface of the SiO_2-rich layer.
5. The glass continues to dissolve, as the ACP layer incorporates (OH) and $(CO_3)_2$ from the solution and crystallizes as an HCA layer.

The first five reaction stages that occur on the glass side of the interface do not depend on the presence of tissues rather they can occur in TRIS-buffer solutions or simulated body fluid (SBF) and have been well studied (Hench *et al.* 1992). Following the glass reaction, the tissue/material interaction takes place as shown in Figure 2. The reaction layers, formed at the surface, enhance adsorption and desorption of growth factors (Stage 6) and influence the length of time macrophages are required to prepare the implant site for tissue repair (Stage 7) and the attachment (Stage 8) and synchronized proliferation and differentiation of osteoblasts (Stage 9). Mineralization of the matrix (Stage10) follows soon thereafter and mature osteocytes, en-

cased in a collagen-HCA matrix, are the final product by 6–12 days *in vitro* and *in vivo* (Hench 2006). The later stages depend on the presence of tissues.

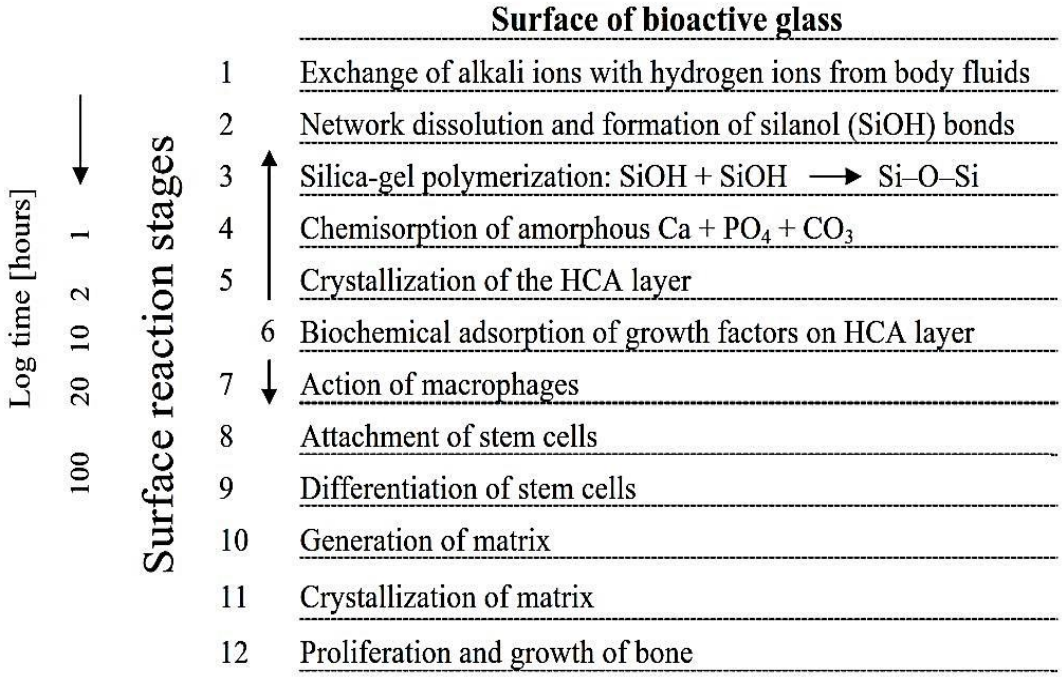

Figure 2: *Sequence of interfacial reactions involved in forming a bond between bone and a bioactive glass (Gerhardt et al. 2010)*

In this thesis, the study is mainly focused on the glass/solution interaction. Dissolution of the newly developed glasses was studied in TRIS buffer solution and in SBF. The TRIS has the advantage over SBF that it is not supersaturated toward the precipitation of HA (Bellucci *et al.* 2011). Thus, studying the dissolution in TRIS allows to further understand the speed of release and layer formation induce by the natural dissolution of the glass. The SBF allows to increase the speed of reaction by mimicking the composition of the extracellular part of the blood plasma (Kokubu *et al.* 2006).

2.1.2 Borate and borosilicate bioactive glass

Borate and borosilicate bioactive glass have been prepared, in the past, by varying the composition of the silicate based glass by adding boron (partially or fully replacing SiO_2 with B_2O_3 (Fu *et al.* 2010, Yao *et al.* 2007). When compared to silicate glass, borate bioactive glass was found to degrade faster and completely convert to HA because of their low chemical durability (Huang *et al.* 2006). The degradation of borate bioactive

glasses (without SiO_2 in the glass structure) follows a congruent mechanism (Liang *et al.* 2007, Yao *et al.* 2007). All ions are leached at the same rate, thereby maintaining the base glass composition. In the case of borate bioactive glasses, no Si nor B-rich layer is form and the HA layer is found to attach directly to the glass surface (Huang *et al.* 2006). At biological pH (7.4 ± 0.2), $B(OH)_3$ is the stable species in aqueous solution. HPO_4^{2-} and $H_2PO_4^-$ are the stable phosphate species. As borate bioactive glasses dissolve in simulated body fluid, the solution pH increases, which would lead to greater amounts of HPO_4^{2-} and $B(OH)_4$ (George 2015). As boric acid is a weaker acid than phosphoric acid, release of BO^{3-} ions from the glass, coupled with the consumption of PO_4^{3-} ions from the solution and the release of the alkali ions results in an increase of pH of the solution (Fu *et al.* 2010). Although borate glasses have shown to help in cell differentiation and cell adhesion *in vitro* (Huang *et al.* 2006), toxicity of borate cannot be neglected. But studies done on rat with borate bioactive glass have shown the toxicity at an acceptable rate (Zhang *et al.* 2010). It is supposed that B ions released from borate glass with lower concentration < 1.792 mM have little, if any, effect on the cell proliferation (Niing *et al.* 2007). The degradation rate of borate bioactive glass can be controlled by replacing SiO_2 with B_2O_3 in silicate bioactive glass (Huang *et al.* 2006). If the composition of these glasses can be tailored, then matching the degradation rate of borate-based bioactive glass with the bone regeneration rate should be possible (Rahaman *et al.* 2011).

2.2 Buffers and Bioactivity

The ability of bioactive glass to form a chemical bond with bone is generally termed as bioactivity. *In vitro* reactions of bioactive glasses are generally studied in buffered inorganic solutions under static conditions to evaluate whether CaP precipitates on the sample. CaP precipitation has been used as an indication of *in vivo* bioactivity (Kokubu *et al.* 2006). The CaP layer is formed by migration of Ca^{2+} and PO_4^{3-} groups to the glass surface and by incorporation of soluble calcium ions and phosphates from the solution or simply by precipitation from appropriate solutions (Hench *et al.* 1991). The CaP layer crystallizes into HA as time progress (Hench *et al.* 1991). These studies are generally performed in TRIS and SBF buffers. On immersion of a bioactive glass in these buffers, three general processes occur: leaching, dissolution and precipitation (Kokubu *et al.* 2006). Fast leaching results in an increase in the pH of the surrounding solution. The pH change varies depending on the glass composition, surface area to volume ratio and agitation rate of the system. By studying the pH change in the solution, a fast and simple determination of the *in vitro* behavior of the glass can be obtained. Though these buffer reactions with bioactive glass is comparable to *in vivo* bioactivity, it should be noted that in *in vivo* condition bioactive glass is exposed to more complex environment of proteins and cells.

2.2.1 SBF

SBF is a type of buffer solution that closely resembles the ion concentration of human blood plasma, with pH of 7.40 and temperature maintained at 37°C (Kokubu *et al.* 1990). The ion concentration of SBF compared to human blood serum is given in table 2 (Kokubu *et al.* 2006). Materials that form apatite at their surface upon dissolution in SBF can bond to living bone if it does not contain any substance able to induce toxic or antibody reaction (Kokubu *et al.* 2006).

Table 2: *Ion concentrations of human blood plasma, SBF and TRIS (mmol/L)*

Ion concentration	Human blood plasma	SBF	TRIS
Na^+	142.0	142.0	-
K^+	5.0	5.0	-
Mg^{2+}	1.5	1.5	-
Ca^{2+}	2.5	2.5	-
Cl^-	103.0	147.8	45
HCO^{3-}	27.0	4.2	-
HPO_4^{2-}	1.0	1.0	-
SO_4^{2-}	0.5	0.5	-

However, one should be aware that thermodynamical calculation led to the conclusion that SBF is saturated toward the precipitation of apatite crystal. Thus, change in the ionic concentration in the solution may induce precipitation of a Ca-P layer while the biomaterial tested is not bioactive (Bohner & Lemaitre 2009). It is therefore crucial to confirm the inherent precipitation of a Ca-P layer using an alternative immersing solution.

2.2.2 TRIS

TRIS buffer has been used as a biochemical buffer to study the dissolution behavior of bioactive glass (Rohanova *et al.* 2011). TRIS buffer has shown to increase the glass dissolution rate because in TRIS, the amino group acts as a ligand for metal ions able to form TRIS-complexed species (Rohanova *et al.* 2011). Surface reactions of various bioactive glass in TRIS buffer solution has been studied earlier (Fagerlund *et al.* 2013, Varila *et al.* 2012) that has shown higher rate of dissolution of bioactive glass in TRIS.

The ions present in the TRIS buffer solution as compared to human blood plasma and SBF as shown in table 2. However, as no other ions are present in the solution all the elements detected in solution upon immersion of the biomaterials can only come from the material's dissolution by products.

2.3 Hot forming, Sintering and Crystallization

There are various stages in manufacturing of the glass. The first stage consists in mixing the raw material. Each raw material is weighted and mixed in proportion such to obtain the expected composition. The second stage is the melting of the raw materials in the furnace. The third stage is glass forming, giving the glass required shape as per its application. Finally, due to the processing and high temperatures involved in the glass processing, there are bound to be thermal stresses in the glass that has been manufactured. Therefore, annealing is done to remove the residual stress (Wallenberger & Smrcek 2010). The manufacture of glass is based on cooling the melt so that it will not attain the crystalline low-energy state it strives to assume. The temperature at which super cooled liquid turns into glass is called the transition temperature or the glass transformation temperature T_g. The liquidus temperature (T_L) is the temperature below which a single liquid phase is no longer thermodynamically stable (Rawson 1980).

The way in which the viscosity of a glass changes with temperature is a crucial factor determining which forming operations can be used to manufacture at medium to high temperature different glass articles. Viscosity of molten glass increases gradually with decreasing temperature and approaches an infinite viscosity value as the melt solidifies (Arstila 2008). The relation between temperature and viscosity of different bioactive glass has been studied (Vedel *et al.* 2007), as shown in figure 3. In the melting furnace the viscosity of the glass melt is in the range of $10 – 10^2$ dPa·s. The commercially important silicate glasses require melting temperatures of at least 1400 °C to reach this viscosity. The melting times are usually several hours in order to ensure homogeneity. A viscous melt can then be transformed to a glassy state by rapid cooling called quenching (Arstila 2008).

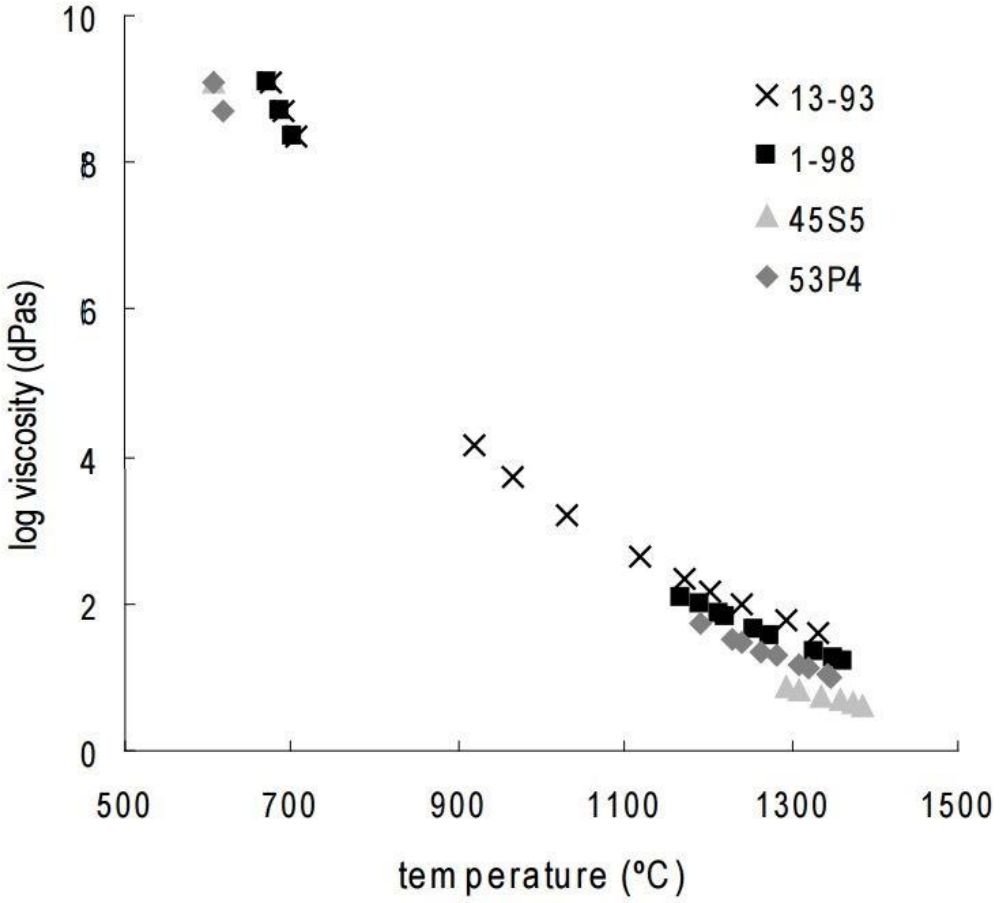

Figure 3: *Viscosity dependence on temperature of different Bioactive glass (Vedel et al. 2007)*

Differential thermal analysis (DTA) is often used to determine the characteristic temperatures associated with particular transitions that occur during heating of glasses. During analysis the temperature is varied linearly as a function of time and the difference between the glass specimen and an inert reference is measured. The first measurable effect is the glass transition temperature T_g, which occurs at a fairly low temperature. The temperature T_g corresponds to the inflection point of the first endothermic event, as shown in Figure 4, that is caused by the increase in heat capacity. At a slightly higher temperature an exothermic peak is usually observed, which is due to crystallization (Arstila 2008). T_x, often refers to the onset of crystallization, while T_p corresponds to the temperature at which the crystallization peak is maximum. The difference in temperature between the T_g and T_x gives the stable temperature for hot forming operations. The wider the range, the easier is the manufacture of bioactive glass products without inducing crystallization. Crystallization is known to affect not only the optical properties of glasses but also their bioactivity (Massera *et al.* 2014b). Thus, an understanding of the effect of chemical composition on the thermal properties of the glass is important when developing bioactive glasses, for which hot forming may reveal beneficial in tis-

sue engineering (Vedel *et al.* 2007). Most glass-forming melts show some sign of crystallization if held just below the liquidus temperature long enough for structural arrangements to occur. Crystallization can occur either on cooling or reheating, but it always involves two individual kinetic processes: formation of submicroscopic nuclei, and their growth into macroscopic crystals. These two processes are called nucleation and crystal growth, respectively (Arstila 2008). XRD technique is used to detect the growth of crystals in the glassy matrix. The XRD pattern of an amorphous material is distinctly different from the crystalline material and consists of few broad diffuse haloes rather than sharp peaks (Padmaja & Kistaiah, 2009).

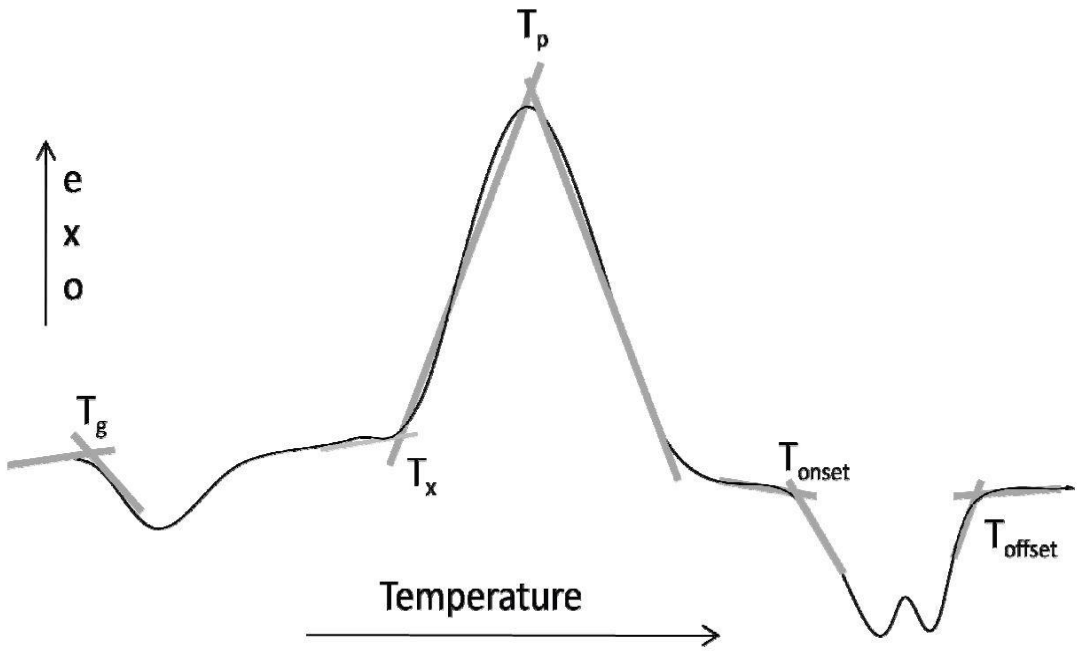

Figure 4: *Ideal DTA curve for the glass represented schematically*

Sintering is the process of making a compact and porous mass from the powder form by spontaneous adhesion (figure 5). Sintering takes place in two stages (Ristic *et al.* 2006). In the first stage, particles of the powder, which is sintered, are combining. During that process the contact surface between particles increases, which in the end results in forming pores in the system. In the second stage, the process of pores overrunning is taking place. That's when pores, representing an infinitely huge concentration of point-defects-vacancies, are decreasing due to diffusion. Sintering mechanism basically takes place as a result of viscous flow.

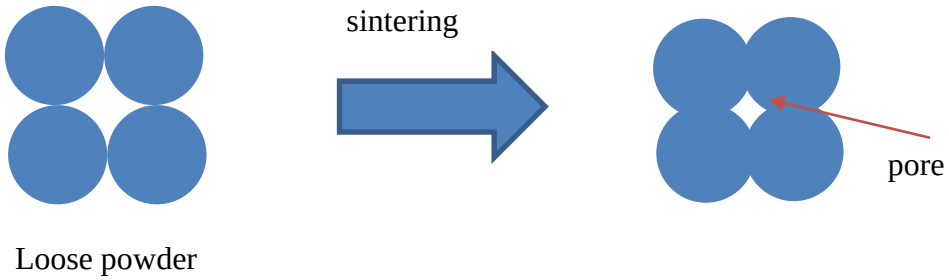

Figure 5: *Schematic diagram showing pore formation during sinte**ring***

Unlike traditional glasses, bioactive glasses have very low silica content which makes them vulnerable to crystallize easily at viscosity ranges typically applied in glass forming. Indeed, it was found that heat sintering of the most commercially bioactive glasses leads to extended surface crystallization in the best case and to phase-separation prior to crystallization in the case of the glass 45S5 (Massera *et al.* 2012). Upon crystallization, typical silicate bioactive glasses showed a decrease in the bioactivity (Fagerlund *et al.* 2012a) while crystallization in phosphate bioactive glasses led to complete loss of the bioactive properties (Massera *et al.* 2015). Sintering compositions tolerating thermal treatments in the sintering range without crystallization are used for making porous implants by viscous flow sintering. The working range for bioactive glasses could be enlarged by decreasing the amount of alkali oxides and by increasing the amount of alkaline earth oxides (Arstila 2008).

2.4 Scaffold, porosity and Mechanical property

Porous scaffolds in tissue engineering play an important role in controlling cell function and regulating new organ formation (Chen *et al.* 2002). There have been several design criteria as defined by Chen *et al.* 2002 for making a general tissue engineered scaffold.

- The surface should permit cell adhesion, promote cell growth, and allow the retention of differentiated cell functions
- The scaffolds should be biocompatible and the bioactive glass nor its degradation or leachates should provoke inflammation or toxicity *in vivo*.
- The scaffold should be biodegradable and eventually dissolve inside the human body.
- The porosity should be high enough to provide sufficient space for cell adhesion, extracellular matrix regeneration, and minimal diffusional constraints during culture, and the pore structure should allow even spatial cell distribution throughout the scaffold to facilitate homogeneous tissue formation.
- The material should be able to be processed into 3D structure and it should be mechanically strong for intended use.

Clinical demand for artificial bone graft materials or bioactive scaffolds that can stimulate bone regeneration by acting as temporary templates for vascularized bone growth

has been increasing. For better osteogenesis, the scaffold should have an interconnected pore structure, with interconnected pore sizes that are greater than 100 μm (Jones *et al.* 2003) but subsequent studies have shown better osteogenesis for implants with pores >300 μm (Tsuruga *et al.* 1997). Larger pores favor direct osteogenesis, since they allow vascularization and high oxygenation but mechanical properties are compromised in larger pore scaffold. Despite its osteoconductive potential and superior ability to bond to bone, the direct application of bioactive glass in load-bearing situations has been limited. Even though existing bioactive materials possess high compressive strength, they are very brittle and have inherently poor tensile and torsional properties (Lu *et al.* 2003). The theoretical strength of flawless solid silicate glass is ~35 GPa (Varshneya 2006). The ability of a glass to resist fracture when a crack is present, i.e. fracture toughness, is low. Even small flaws lead to the decrease in strength drastically, and typical strength of common glass products is only around 14-70 MPa (Varshneya 2006). Depending on the composition of the glass, the compressive strength of bioactive silica glasses is around 800-1200 MPa and tensile bending strength is 40 to 60 MPa (Carter & Norton 2007). The compressive strength of cancellous bone is 2-12 MPa and that of cortical bone 100-230 MPa (Heikkilä 2011).

Manufacturing a bioactive scaffold having mechanical properties comparable to a load bearing bone and having anatomically accurate shape with required porosity is a challenging task. There are various methods to prepare a porous bioactive scaffold such as sol–gel, thermally bonding of particles (fibers or spheres), polymer foam replication, freeze casting, and solid freeform fabrication (Fu *et al.* 2011).

- The scaffolds made by sol-gel degrade and convert faster to HA than scaffolds from melt-derived glass with the same composition. However, these sol–gel derived scaffolds have low strength which leads to application only in non-load bearing sites (Jones *et al.* 2006).
- Scaffolds made by thermal bonding of glass particles has advantage of making scaffold of required geometry, also it doesn't require complex machinery but the main disadvantage of this method is the poor pore inter connectivity (Belluci *et al.* 2010).
- The polymer foam replication technique is able to make a scaffold microstructure which is similar to that of dry human trabecular bone. Highly porous glass scaffolds with open and interconnected porosity in the range 40–95% can be produced from this method. Scaffolds of silicate, borosilicate, and borate bioactive glass have been prepared using this method (Chen *et al.* 2006). However, low strength of the scaffold limits its use to the repair of low-load bearing sites.
- Solid freeform prototyping enables precise manipulation of the 3D architecture, and printing of lines as thin as 30 μm using micron-sized glass powders. The sintered glass scaffolds, with an anisotropic structure, show a compressive strength (136 MPa) comparable to human cortical bone, which indicates that these scaffolds have

excellent potential for the repair and regeneration of load-bearing bone defects (Fu *et al.* 2011).

- Freeze casting method can obtain scaffold with high mechanical properties but pore width in the range of 10–40 μm which is too small to support tissue ingrowth. Silicate glass scaffolds of compositions 45S5 glass has been prepared using the technique (Fu *et al.* 2010).

Studies have shown that amorphous porous bioactive glass structures can be sintered from bioactive glasses having a wide hot-working range (Ylänen 2000). Simple heat sintering does not require complex machinery and shapes of the scaffold can be maintained by just inserting the glass in powder form in a mould. Desired mechanical properties and porosities can also be obtained by choosing the right particle size. Taking these advantages of sintering, this thesis uses simple heat sintering method for the preparation of scaffold.

3. MATERIALS AND METHODS

3.1 Preparation of glasses

In this study two set of borosilicate glasses were produced to evidence the impact of boron trioxide on the physical, thermal, structural and *in vitro* properties. In a first time, one mol of Silicon was substituted for one mol of Boron. 0.5, 1, 2, 5 and 10 mol% of SiO_2 was substituted with B_2O_3, in S53P4 glass. The glasses were labelled 0.5B, 1B, 2B, 5B and 10B respectively. In a second time, 25%, 50% and 75% of the total SiO_2 content was substituted with B_2O_3, while maintain CaO, Na_2O and P_2O_5 constant. The glasses were labelled B25, B50 and B75 respectively. The glass S53P4 was used as a standard reference as it has been well studied in the past (Andersson *et al.* 1990, Massera *et al.* 2014a). The composition of the various borosilicate glasses studied is shown in the table 3.

Table 3: *Novel borosilicate glass composition (mol %)*

Elements	S53P4	0.5B	1B	2B	5B	10B	B25	B50	B75
SiO_2	53.86	53.13	52.4	50.94	46.55	39.25	40.40	26.93	13.46
B_2O_3	0.00	0.50	1.00	2.00	5.00	10.00	13.46	26.93	40.40
Na_2O	22.66	22.77	22.89	23.11	23.79	24.93	22.66	22.66	22.66
P_2O_5	1.72	1.73	1.74	1.75	1.81	1.89	1.72	1.72	1.72
CaO	21.77	21.87	21.98	22.20	22.85	23.94	21.77	21.77	21.77
Total	*100*	*100*	*100.01*	*100*	*100*	*100.01*	*100*	*100*	*100*

Glasses were melted from batches containing mixtures of sand (99.4 % pure SiO_2), and analytical grades of Na_2CO_3, H_3BO_3, $CaCO_3$, and $CaHPO_4.2H_2O$. The glasses were melted in air, in a platinum crucible at temperature from 1000 to 1400 ^oC depending on the boron content. The exact melting procedure used for each glasses are listed in Table 4. The glasses were then casted into a graphite mould. Successively the ingots were annealed and crushed into powders with <50 µm, 250-500 µm, >500 µm sizes.

Table 4: *Glass casting protocol used to prepare the glass.*

Glass	Temperature °C	Time Minutes	Annealing Temperature °C
	600	30	
S53P4	1000	30	450
	1450	120	
	600	30	
0.5B	1000	30	450
	1450	120	
	600	30	
1B	1000	30	450
	1450	120	
	600	30	
2B	1000	30	450
	1450	120	
	600	30	
5B	1000	30	450
	1325	90	
	600	30	
10B	800	30	450
	1200	90	
	600	30	
B25	800	40	450
	1100	60	
	1300	120	
B50	600	30	
	800	30	450
	1200	30	

B75	600	30	
	800	45	450
	1150	30	

3.2 Preparation of buffers

Two buffer solutions were used for the glass characterization test: namely SBF and TRIS. The SBF was prepared according to the method described by (Kokubu *et al.* 1990). The chemicals required for the preparation of SBF are given in Table 5. the chemicals were weighed (in the order they are presented in the Table) and introduced in a glass beaker containing about 700ml deionized water which was continuously magnetically stirred. The reagents were added one after the other ensuring that the previous reagent was fully dissolved. Trizma base was carefully mixed in the solution 0.5 mg at a time until it fully dissolved. The solution was let to rest for 4 h in a water bath before adjusting the pH to 7.40 at 37ºC by titrating the solution with 1N HCl. The solution was poured in a glass flask and deionized water was added to obtain 1 liter of SBF. The flask was shaken and stored in the refrigerator and used within 20 days.

Table 5: *Reagents used to prepare SBF*

Order	**Reagent**	**Amount**
1	NaCl	7.996 g
2	$NaHCO_3$	0.350 g
3	KCl	0.224 g
4	K_2HPO_4	0.228 g
5	$MgCl_2.6H_2O$	0.305g
6	1N-HCl	35 ml
7	$CaCl_2$	0.278 g
8	Na_2SO_4	0.071g
9	$(CH_2OH)_3NH_2$ (Trizma Base)	6.057 g

TRIS buffer was prepared as described by Sigma Aldrich to obtain 1 liter of TRIS buffer pH 7.40 at 37°C. About 400 ml deionized water was taken in a clean beaker which

was continuously magnetically stirred. The reagents (from Sigma Aldrich) listed in table 6 was put one after another each reagent about 0.5 g at a time until it fully dissolved. Then the solution was left for about 1 hour for thorough mixing. The temperature was maintained at 37°C. The solution was then transferred to the 1-liter flask and 1 liter of buffer was prepared by adding deionized water and stored in the refrigerator before use. The buffer solution was used within 20 days.

Table 6: *Reagents used to prepare TRIS buffer*

Order	Reagent	Amount
1	Trizma base	1.66 g
2	Trizma HCL	5.72 g

3.3 Density

The density of bulk glass materials was measured by Archimedes' principle using deionized water. Three repetitions were carried out and average measurements were calculated. The accuracy was better than 0.03g/cm^3.

3.4 Glass structural analysis

Fourier transformed infrared spectroscopy (FTIR) in attenuated total reflectance mode was employed to evidence the structural change induced by the replacement of SiO_2 by B_2O_3 as well as the structural and surface morphology change induce by the glass reaction in SBF and TRIS. FTIR was performed using a Perkin Elmer Spectrum one FTIR spectrometer. The resolution used was 4cm^{-1}, and the number of accumulated scan was 8.

3.5 Thermal analysis

The glass transition temperature T_g, the onset of crystallization T_x and the crystallization temperature T_p of the glasses were determined using differential thermal analysis at heating rates 10°C/min for glass particle sizes <50 µm (fine powders) and 250–500 µm (Coarse powders). The glass transition temperature was taken at the inflection point of the endotherm, as obtained by taking the first derivative of the DTA curve. The crystallization temperature T_p was found at the maximum of the exothermic peak. The accuracy of the measurements was ± 3°C. The measurements were performed on 30 mg samples in platinum pans and in an N_2 atmosphere.

3.6 *In vitro* testing

Glass particulates with grain size < 50 μm and 250-500 μm were immersed in 50 ml of simulated body fluid (SBF) and TRIS for 6, 24, 48, 72, and 168 h at 37 ºC in an incubating shaker (INFORS Multitron II). Two parallel samples were taken for each test point. In the shaker, the orbital speed of 100 RPM was chosen to give laminar flow mixing of the solution without inducing particle movement. The mass of sample immersed in the solution was adjusted to give a constant surface area to volume ratio (SA/V≈9.1 X 10^{-2} cm^2/ml). As the glass was crushed by hand and then sieved, the SA was calculated assuming similar average particles size and correcting for the glasses density. The mass used varied from 75mg for the S53P4 glass to 72.6 mg for B75 glass. The change in the solution pH was recorded for each immersion time and average of the parallel samples was calculated. The pH was compared to a blank sample containing only SBF or TRIS. After testing, the powder was washed with acetone and dried. The composition and structure of the glass powder were analyzed in FTIR.

3.7 Scaffold processing

A stainless steel mould with 20 holes (10 mm depth and 5mm diameter) was used to prepare the scaffolds. Boron nitride paste was used to coat the internal holes of the mould so that the sintered glass particles did not stick in the mould. The effect of sintering temperature and particle size on the porosity was studied on the most promising glasses. The sintering time was maintained constant to 1 hour.

3.8 Mechanical testing of the scaffold

Compression testing was performed for the scaffold with the most promising characteristics in Instron 4411 machine. Three sets of parallel sample were used in the test with load cell of 500N and crosshead speed of 0.5mm per minute. The mean and standard deviation of the compression strength was calculated.

4. RESULTS AND DISCUSSION

4.1 First glass series

Glasses with the oxide composition in mol% $53.85SiO_2$-xB_2O_3-$22.66Na_2O$-$1.72P_2O_5$-21.77CaO with x varied as (0, 0.5, 1, 2, 5, 10) and maintaining other oxide composition according to mole variation in B_2O_3 were labelled S53P4, 0.5B, 1B, 2B, 5B, 10B respectively. These glasses were prepared using a standard melting.

4.1.1 Density

The density of the glass was measured by the Archimedes principle. With an increase in the boron content, no noticeable change in the density could be measured, within the accuracy of the measurement. The density of all glasses was found to be (2.64 ±0.03) g/cm^3. The molar volume which represents the space occupied by one mol of glass can be expressed as $V_m=M/\rho$ where M is the molecular mass and ρ the density. With an increase in the boron content, the molar volume decreases indicating that the network contracts either due to the formation of Si-O-B bonds or due to the formation of a borate sub-structure within the silicate network.

4.1.2 Structural properties

The FTIR spectrum of the investigated glasses is shown in figure 6. All the spectrum where background corrected and normalized to the band with maximum intensity. The spectrum of the boron-free glass, S53P4, shows absorption bands at 748, 930, 1023 cm^{-1} and in the 1400–1515 cm^{-1} region. The band at 930 cm^{-1} can be attributed to Si–O^- and the band peaking around 1023 cm^{-1} to Si–O–Si asymmetric stretching in SiO_4 units. The band at 748 cm^{-1} is due to Si–O bending and the band located within the 1400–1515 cm^{-1} range is related to carbonate in the glass structure.

When the boron content increases, new bands appear at 715, 1227 and 1401 cm^{-1}. The new band formed at 715 cm^{-1}, the intensity of which increases with an increase of boron content, can be attributed to B-O-B bending (Serra *et al.* 2003, Queiroz *et al.* 2003, Pascuta *et al.* 2008). The position of the band at 1401 cm^{-1} shifts to 1380 cm^{-1} when the boron content increases. This band, as well as the shoulder at 1337 cm^{-1} have been related to borate triangles BO_3 and the band at 1227 cm^{-1} to BO_2O^- (Serra *et al.* 2003, Pascuta *et al.* 2008). One can notice that the two bands at 930 and 1023 cm^{-1} broaden with an increase in boron content and have been attributed to a combination of vibration modes from BO_4 units, B-O-Si and B-O-B linkages, respectively (Serra *et al.* 2003,

Queiroz *et al.* 2003, Pascuta *et al.* 2008). Additionally, the band at 748 cm^{-1} related to Si-O bending decreases in intensity and a new band at 715 cm^{-1} appears and increase in intensity. This last band was attributed to B-O-B bending vibration (Serra *et al.* 2003, Queiroz *et al.* 2003, Pascuta *et al.* 2008).

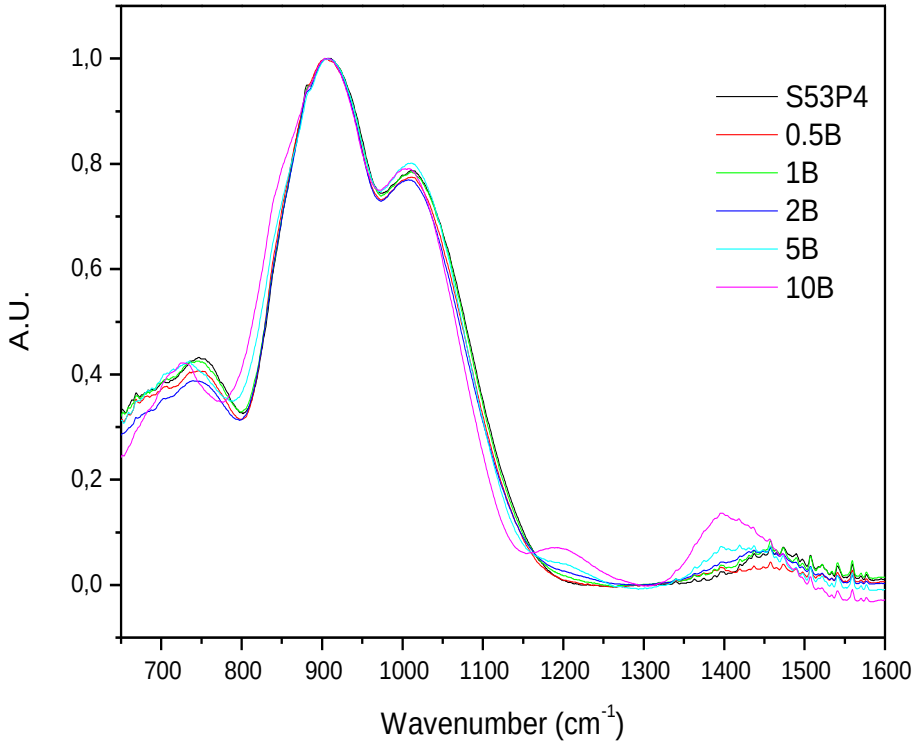

Figure 6: *FTIR spectra of the first series of glasses*

In summary, from the analysis of the FTIR spectra, it is possible to think that with an increase of the boron content, the glasses' structure forms two separate sub-structures: one rich in SiO_2 and one rich in B_2O_3.

4.1.3 Thermal properties

The DTA thermograms of the glass powders are presented in Figure 7 for the coarse powder and Figure 8 for the fine powder. The measurement was performed on both particles size as, often, change in the crystallization peak shape and intensity with respect to the granule size gives information on the crystallization mechanism (Massera *et al.* 2012)

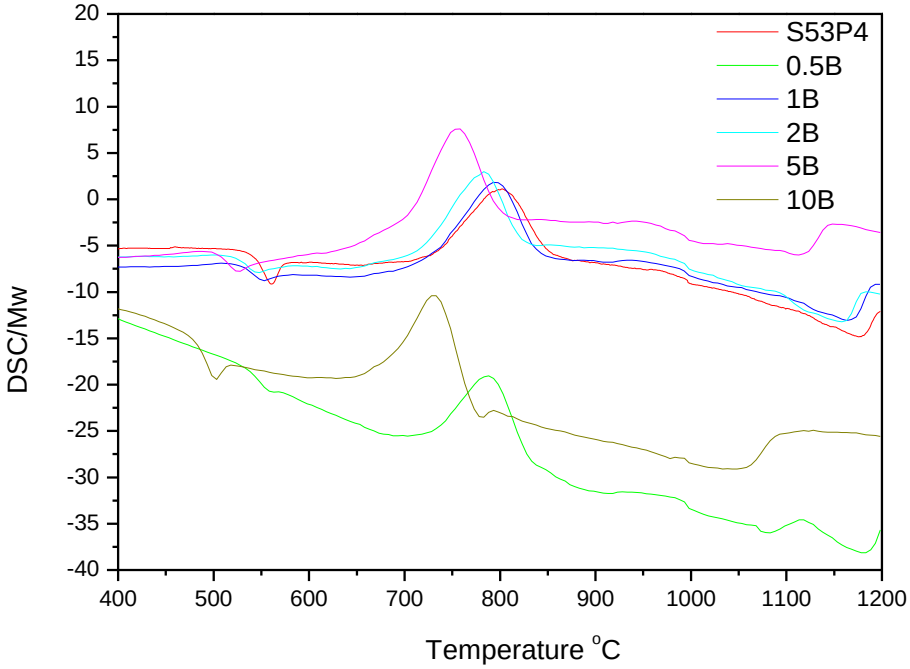

Figure 7: *DTA of coarse glass powders*

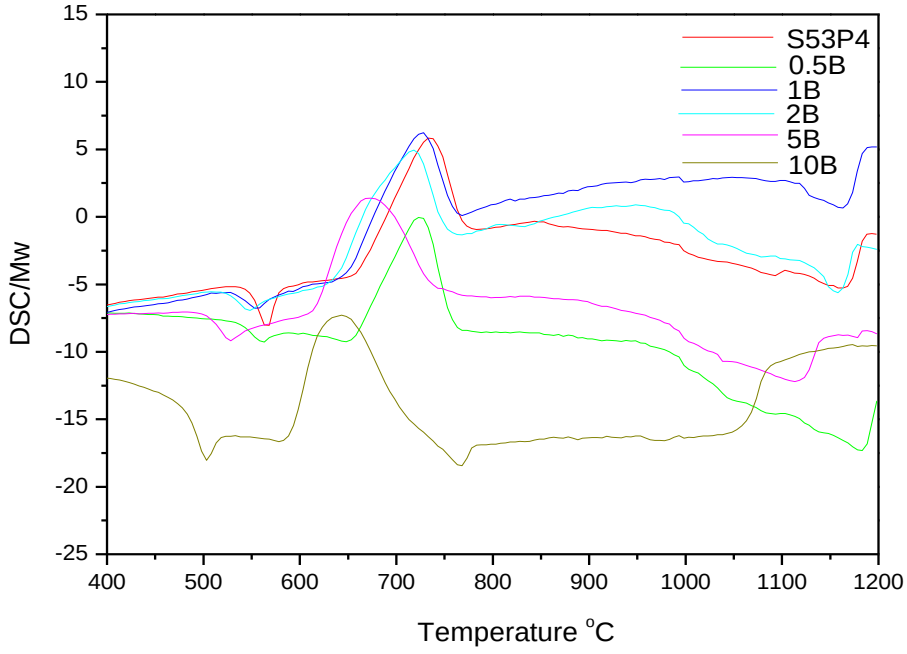

Figure 8: *DTA of fine glass powders*

From the DTA thermogram the T_g, T_x and T_p was extracted and are reported in Figure 9 and 10 for the coarse and fine powder respectively. T_g is represented on the left Y-axis, T_x and T_p in the right Y-axis.

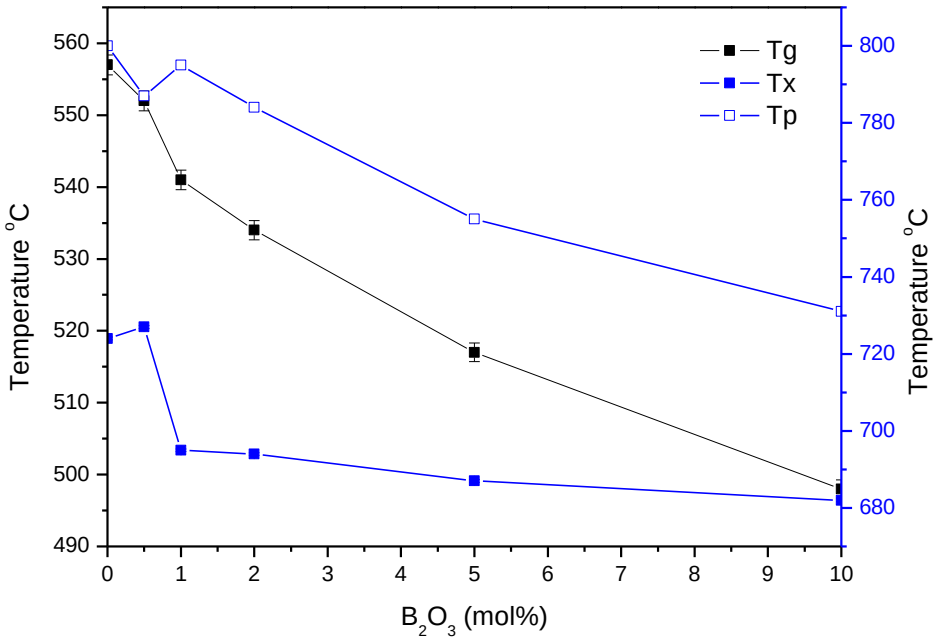

Figure 9: *T_g, T_x and T_p of first series of coarse glass powder*

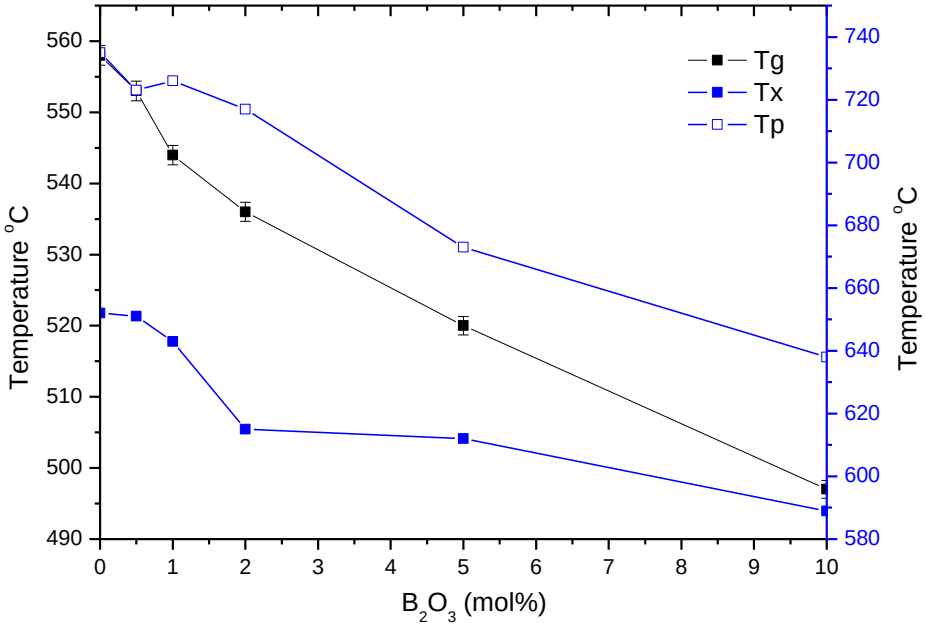

Figure 10: *T_g, T_x and T_p of first series of fine glass powder*

With an increase in the boron content the T_g, T_x and T_p decreases. This is in agreement with previous studies which showed that B_2O_3 can be used to decrease the T_g and forming temperatures of glasses (Brink *et al.* 1997). Also with decreasing the particle size,

all characteristic temperature was found to shift toward lower temperature. This is due to the thermal lag effect (Massera *et al.* 2012). Indeed, smaller particles size, have smaller volume which would "see" the furnace temperature at earlier time than large particles.

Changes in the shape of the exothermic peak, such as bandwidth and intensity, are usually indications of a change in the crystallization mechanism (Massera *et al.* 2012). The height of the peak for the investigated glasses is shown in the table 7. One can observe that with an increase in boron content, the intensity of the crystallization peak decreases. However, the intensity of the peaks did not vary greatly when using fine particles rather than large particles. This indicates that the crystallization mechanism of these glasses is not particle size dependent (Massera *et al.* 2012).

Table 7: *Comparison of height of crystallization peak of glass powders*

Glass	Peak (A.U.)	
	Coarse Powder	Fine powder
S53P4	6.68	6.43
0.5B	6.45	6.12
1B	6.06	5.75
2B	5.94	5.34
5B	5.73	5.35
10B	5.34	5.21

Figure 11 shows ΔT, as a function of boron content, which is the difference between T_x and T_g. ΔT represents the stability of the glass against crystallization. It can be seen that ΔT increases with an increase in boron content indicating that the progressive addition of boron increases the glass stability against crystallization. However, one can notice that ΔT measured from fine glass powder is smaller than that of the coarse glass powder. This is an indication that the crystallization might be occurring form the surface thus coarse particle should be used during sintering of these glass in order to avoid significant glass crystallization.

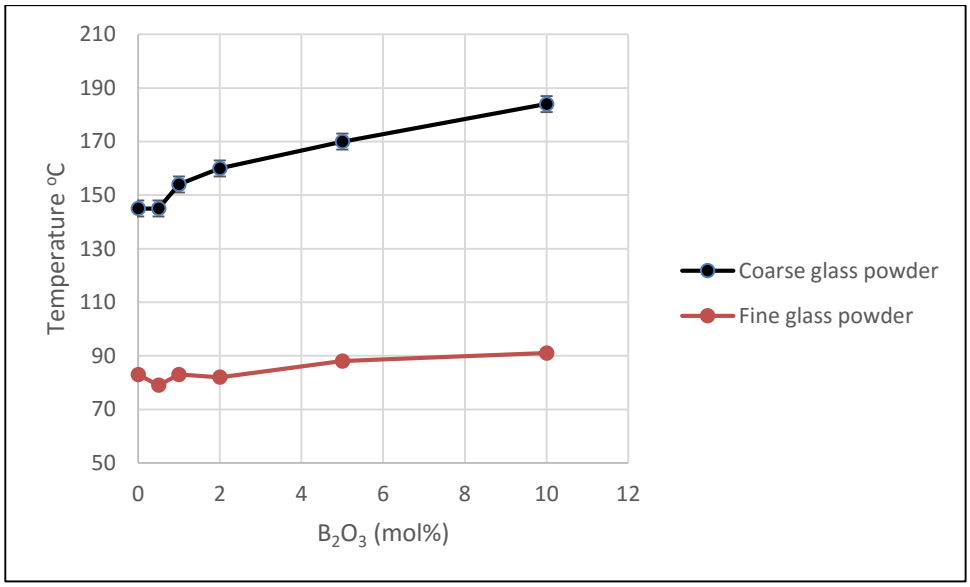

Figure 11: *Hot forming range for the first series of coarse glass powder*

4.1.4 *In vitro* dissolution studies

The first step of the *in vitro* study was performed in simulated body fluid for the coarse and fine powder. Figure 12 presents the change in pH as a function of the time of immersion of the coarse powder whereas Figure 13 presents the change in pH when the fine particles are immersed.

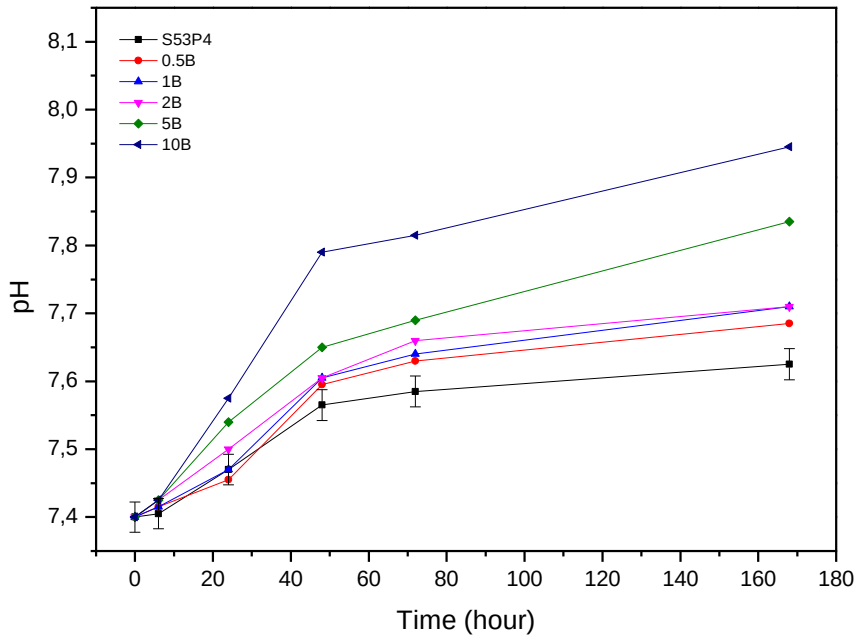

Figure 12: *pH values of coarse glasses in SBF over time. Each point represents mean for two parallel samples.*

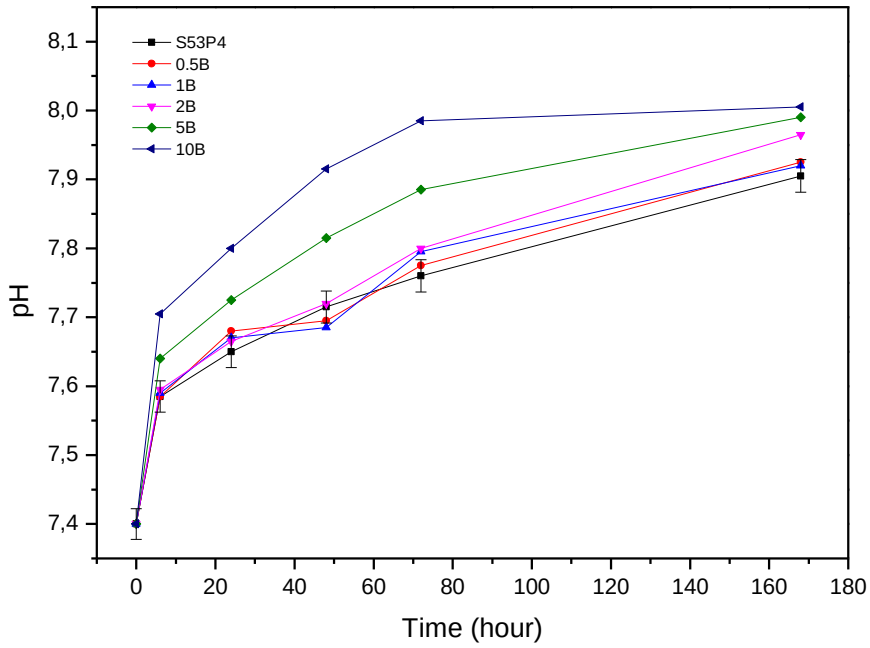

Figure 13: *pH values of fine glass in SBF over time. Each point represents average for three parallel samples.*

In both graphs, an increase in the pH can be seen with increasing the immersion time. As explained in the previous section, this can be attributed to the release of alkaline and alkaline earth ions from the glass to the solution increasing the solution basicity. With an increase in the boron content, the pH rises faster indicating that the initial dissolution rate of the boron-containing glasses is faster than the boron-free glass. The boron sub-network is believed to dissolve at a faster rate than the silicate phase. Indeed, borate glasses are known to have faster dissolution rate than the typical silicate bioactive glasses (Huang *et al.* 2006). When comparing the pH change of the coarse and fine powder samples, it is noticeable that the final pH is higher when fine powder is used for the experiment. This can be attributed to the higher surface area to volume ratio which leads to increased surface in contact with the solution. This in turn implies a faster dissolution of the material.

It is noteworthy that in Figure13, whereas the initial dissolution is greatly higher for the glasses labelled 5B and 10B, the final pH does not differ so markedly. Even more, it seems that the pH of the B10 glass saturates at 72h of immersions.

As it is known that SBF is thermodynamically unstable and saturated toward the formation of apatite (Kokubu and Takadama 2005), it is conceivable that upon immersion a HCA layer precipitate at the glasses surface. To better understand the dissolution rate of the glasses a similar test is performed in TRIS buffer solution.

Similar rise of the pH values was observed from the glass powders in the TRIS buffer as evidenced from figure 14 for coarse glass powder and Figure 15 for fine glass powder.

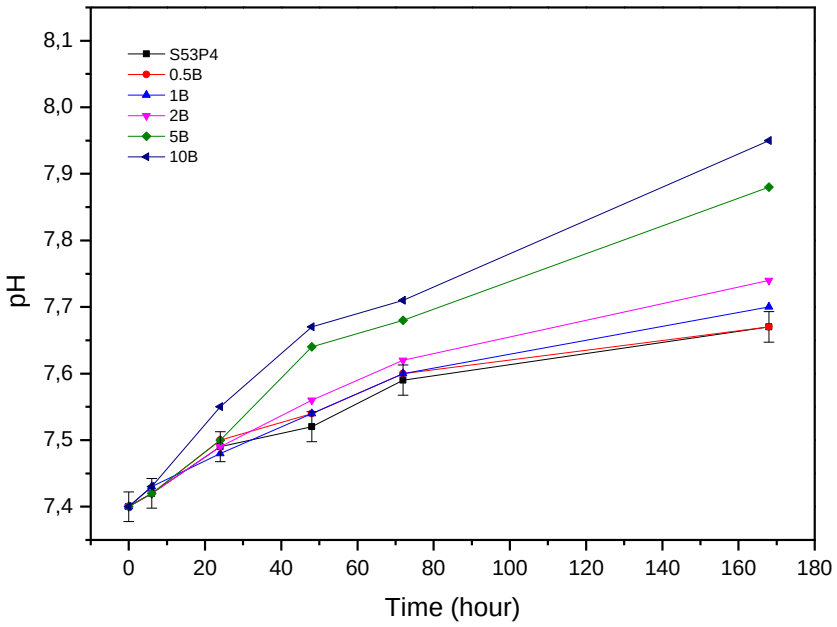

Figure 14: *pH of coarse glass powders in TRIS. Each point represents mean for two parallel samples.*

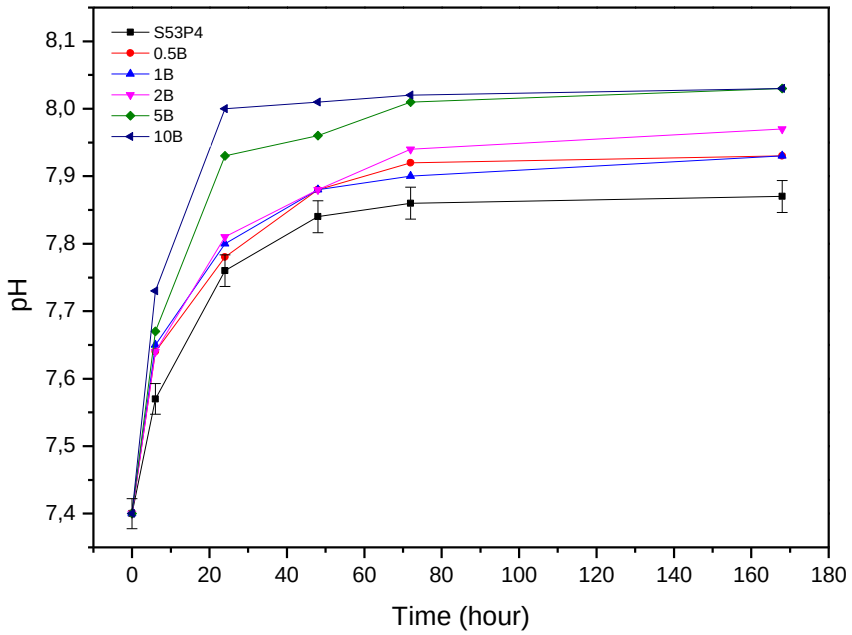

Figure 15: *pH of fine glass powders in TRIS. Each point represents mean for two parallel samples.*

The pH of the coarse glass powders linearly rises during the all duration of the immersion test. The B10 glass exhibits the highest pH value confirming the increase in the dissolution properties of the boron-containing glasses. Similarly, fine powders in TRIS buffer show sharp rise in pH already after 6 hours in TRIS. This is due to the fact that large surface area is in contact with the TRIS buffer releasing more ions into the buffer solution. It is noteworthy that the pH of fine glass powder remains steady after 72 hours in TRIS due, most likely due to the saturation of the TRIS solution with ions leaching out form the glasses. The sharp rise in pH in TRIS is due to a faster dissolution of bioactive glass in TRIS than in SBF, which was also observed by (Fagerlund *et al.* 2013).

Changes in the glass surface composition as a function of immersion time in SBF and TRIS was assessed via FTIR. The spectrum of the S53P4 glass, shown in figure 16, exhibits a decrease in band 950 cm^{-1} as the immersion time increases, revealing a decrease in $Si\text{-}O^-$ and a decrease in SiO_4 unit. The presence of the shoulder at 959 cm^{-1} may be attributed to C–O vibration modes in CO_3^{2-} and to P-O-P bonding (Massera *et al.* 2014a). The presence of phosphate vibrations is further confirmed with the appearance of the shoulder at 875 cm^{-1} which can be attributed to P-O vibration and the increase in intensity of the band at 1350–1550 cm^{-1} attributed to carbonate group (Massera *et al.* 2014a). It is clearly seen that S53P4 forms a carbonated apatite layer when immersed in SBF. Hence, the phosphate vibrations can be related to apatite layer formation (HA) and the increase in the band 1350–1550 cm^{-1} most likely to carbonate substituted hydroxyapatite irrespective of sample glasses (Massera *et al.* 2014a).

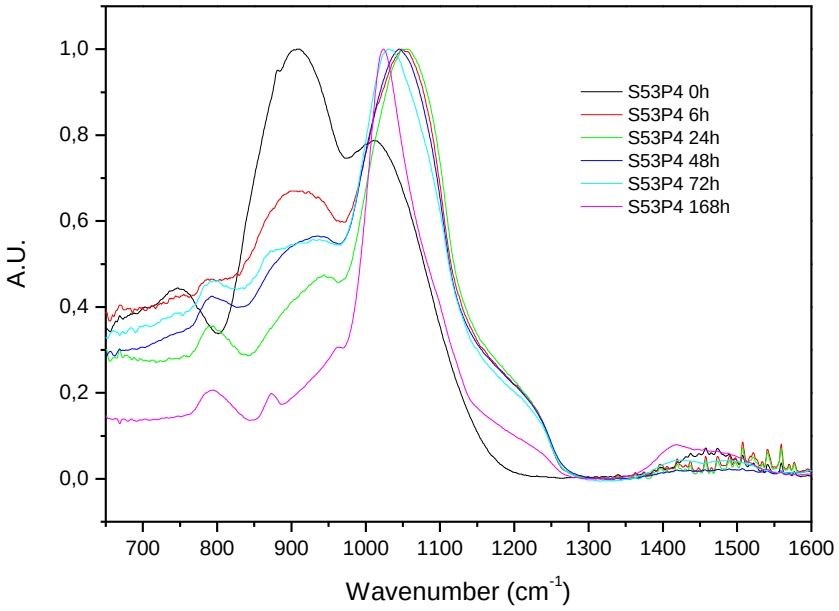

Figure 16: *FTIR of S53P4 fine glass powder immersed at different time in SBF*

The FTIR spectra of S53P4 glass immersed in TRIS is presented in Figure 17. It can be seen that even after one week of immersion clear HA layer is not clearly visible as in the SBF. This is due to the fact that TRIS is not supersaturated toward the precipitation of HA and may also attribute to the slow formation of HA in silicate glasses.

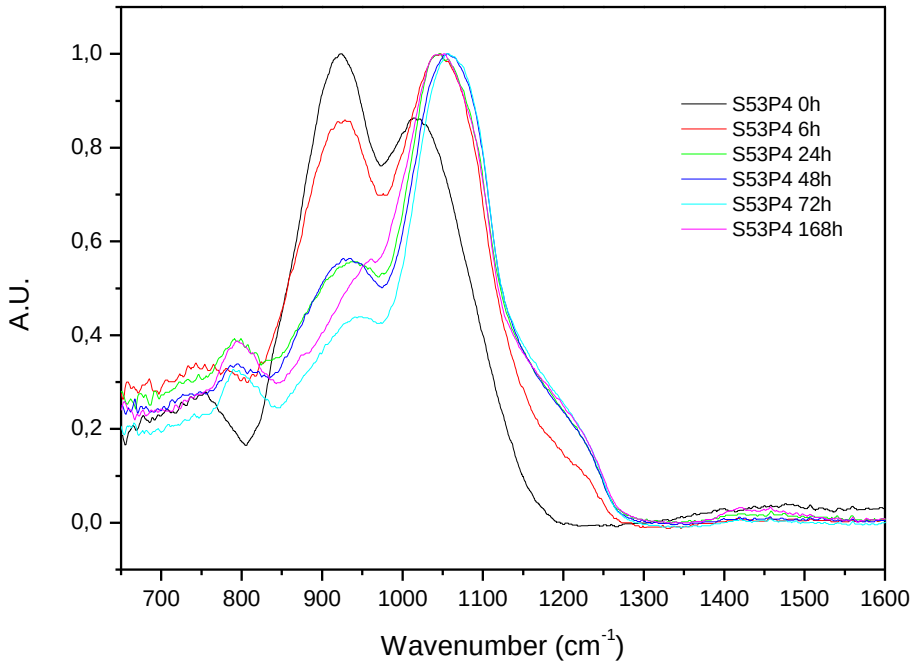

Figure 17: *FTIR of S53P4 coarse glass powder immersed at different time in TRIS*

The FTIR spectra of the boron-containing glasses, after immersion in SBF for 48 and 168h, are presented in figures 18 and 19, respectively. Upon immersion in SBF, the bands in the 1200-1600 cm^{-1} region, corresponding to the borate network, decrease in intensity and a doublet in the 1350-1550 cm^{-1} region appears and increases in intensity with an increase in immersion time. The broad band in the 800-1150 cm^{-1} region splits into three well defined bands centered at 1009, 948 and 872 cm^{-1} after initial immersion. For longer immersion, the band at 1009 cm^{-1} shift to 1019 cm^{-1} while the position of the bands at 948 and 872 cm^{-1} remain stable. These changes in the FTIR spectra overtime show that the B_2O_3 containing glasses show structural modification where the boron network is being hydrolyzed and leached out into the solution with successive precipitation of HCA.

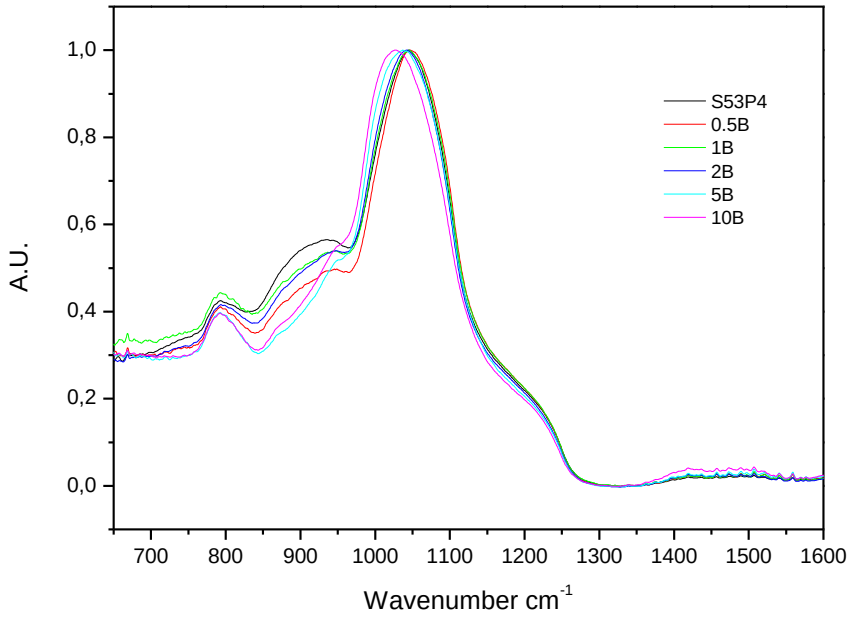

Figure 18: *FTIR of glass powders immersed 48h in SBF*

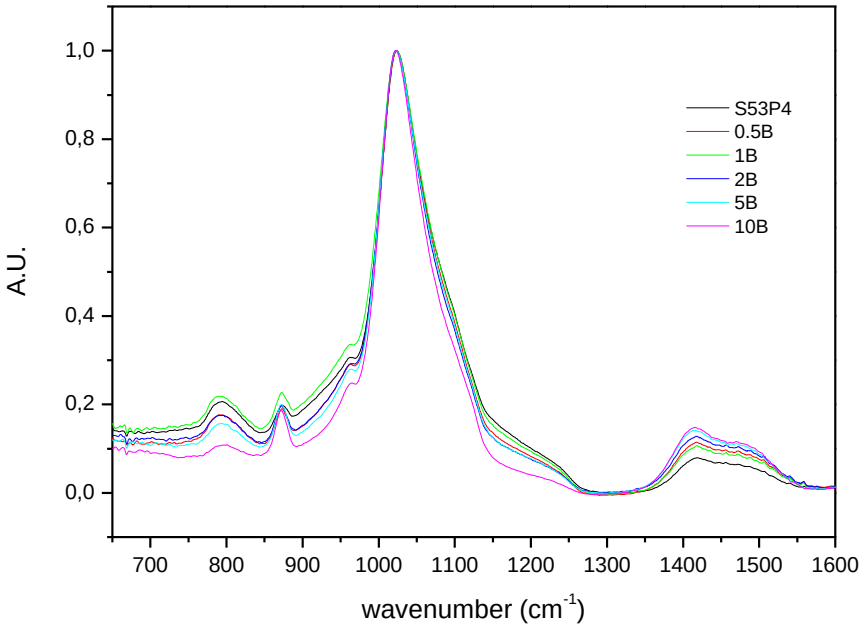

Figure 19: *FTIR of glass powders immersed 1 week in SBF*

One can clearly see that the surface structural modification occurs more rapidly (Figure 18) for the boron containing glasses. HCA is also thicker and more crystallized at the surface of the boron containing glasses as evidence in Figure 19 by the lower intensity of the shoulder at ~1220 cm^{-1} related to the silica gel at the interface between the glass

and the precipitated layer as well as the increase in intensity, with increasing boron content, of the carbonate vibration absorption band (Massera *et al.* 2014a).

Figure 20 and 21 present the FTIR spectra of the glasses immersed in TRIS for 48 and 168h.

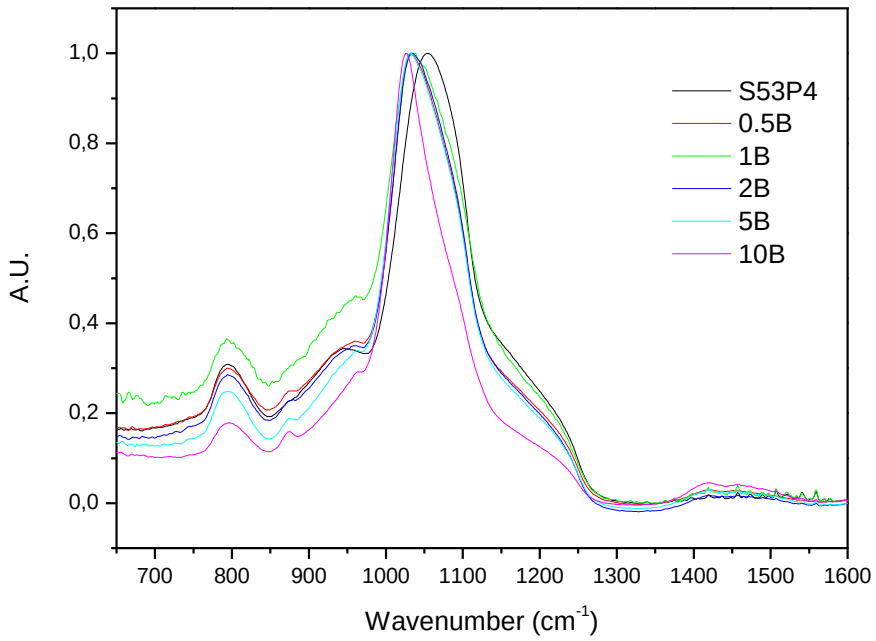

Figure 20: *FTIR of glass powders immersed in TRIS 48H*

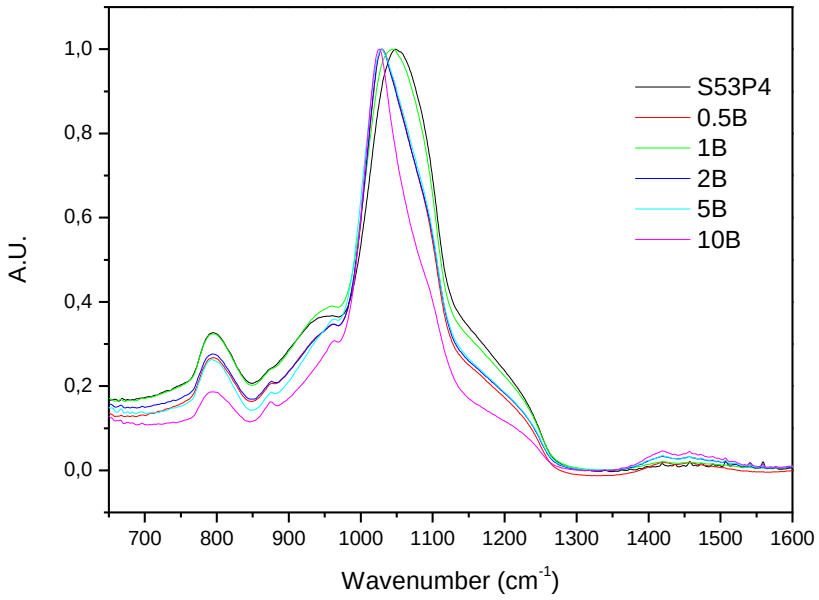

Figure 21: *Glass immersed in TRIS 1 week*

As seen in the case of immersion in SBF at 48h corrosion of the borate and silicate network within the glass takes place and precipitation of a calcium phosphate layer precipitate at the surface of the glass surface. It is clear from Figure 20 that the glass containing boron precipitates more HA at the glass surface as evidence by the shift and sharpening of the main band. However, if at 48 h the absorption related to the vibration of the phosphate units are more intense for glass particle immersed in TRIS, at 168 h the FTIR signals show less pronounced phosphate vibration when immersed in TRIS than in SBF. This is due to the composition of the solutions. The SBF containing a significant amount Ca and P is more likely to be saturate at earlier time and to precipitate a thicker HCA layer. At the contrary the lack of ions in the TRIS buffer solution leads to a more sustain glass dissolution and a delayed layer formation.

4.2 Second glass series

Glasses with the oxide composition in mol% 53.85-xSiO_2-xB_2O_3-22.66Na_2O-1.72P_2O_5-21.77CaO with x varied as 13.46, 26.92 and 40.39 were labelled as B25, B50 and B75. The glasses were prepared using a standard melting. Based on the results obtained from the previous glass series, the study has been conducted on large particle sizes and in SBF.

4.2.1 Density

The change in density and molar volume due to the replacement of SiO_2 by B_2O_3 is shown in the figure 22. The density of the glass decreases from (2.64±0.03) g/cm^3 in S53P4 glass to (2.57±0.03) g/cm^3 while the molar volume increases when the boron content increases from 0 to 75%. Due to the large substitution of SiO_2 with B_2O_3, drastic change in density was recorded. The mass of the sample to be immersed was adjusted to maintain a SA/V = 9.1 10^{-2} cm/ml. The surface area of the samples was calculated based on the density and assuming that the average particle size was independent of the glass composition and the particles are spherical. The increase in the molar volume tends to indicate that with increasing the SiO_2 substitution with sufficient amount of B_2O_3 the glass structure progressively expands. This is due to the fact that the boron ions are likely to form B-O-Si, diborate and non-bridging oxygens (NBOs) in the glass structure leading to an increase in the free volume within the glass network (Shelby 2005). Such behavior was not seen in the earlier glasses as the boron content remained relatively low.

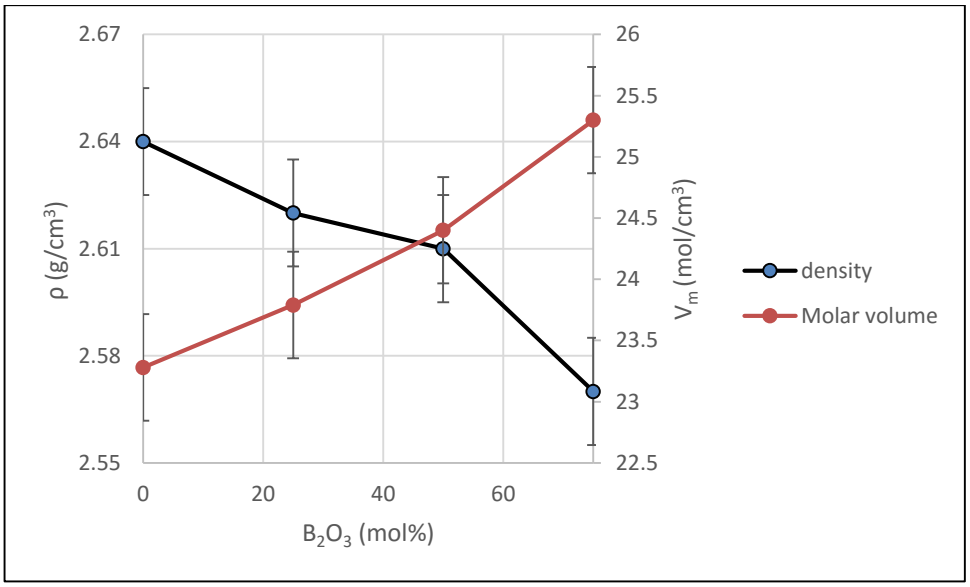

Figure 22: *Density and molar volume of the investigated second series of glass*

4.2.2 Structural properties

The FTIR spectra of the investigated glasses are shown in the figure 23. With an increase in boron content, the band at 748 cm^{-1} related to Si-O bending decreases and a new band appears at 715 cm^{-1}, the intensity of which increases. This band has been attributed to B-O-B bending (Serra *et al.* 2003, Queiroz *et al.* 2003, Pascuta *et al.* 2008). The band around 1380 cm^{-1} is due to the BO_3 triangle and a shoulder at 1337 cm^{-1} and a band at 1227 cm^{-1} appeared due to BO_3 (Serra *et al.* 2003, Queiroz *et al.* 2003, Pascuta *et al.* 2008) after addition of Boron. It is noteworthy that the absorption bands related to the borate network are more intense in this glass system due to the higher boron content compared to the previously presented glass series.

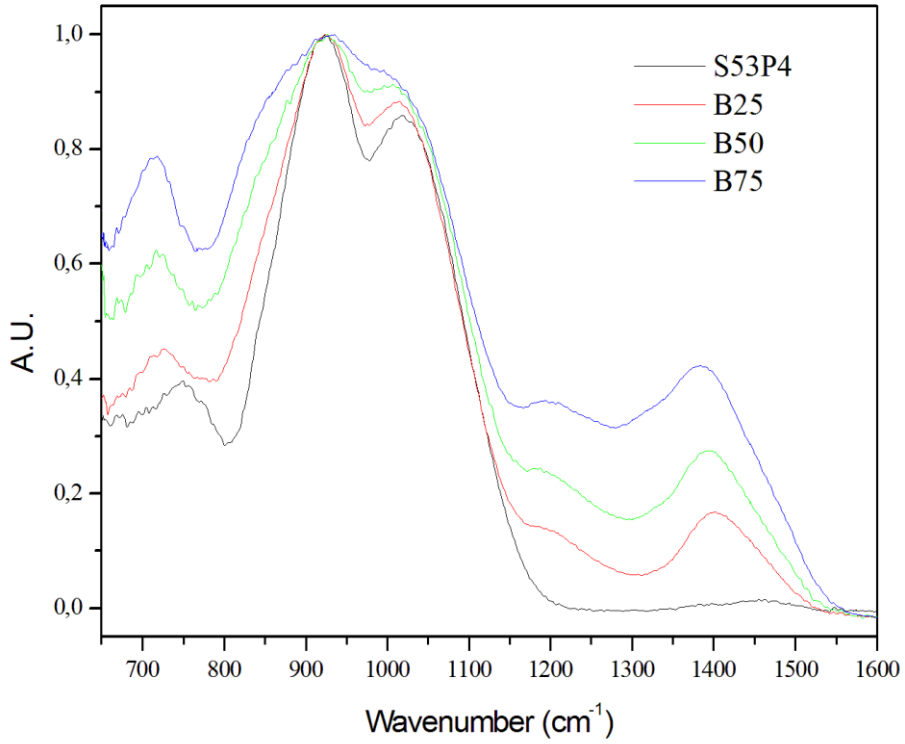

Figure 23: *FTIR spectra of second series of glass powders*

4.2.3 Thermal properties

Figure 24 shows the DTA thermogram of the investigated glasses, for the coarse particles. The coarse powder was chosen based on the analysis of the first series of glass. Indeed, the use of fine or coarse powder did not show significant changes in the crystallization tendency. The characteristic temperature (T_g, T_x and T_p) are reported in Figure 25, with T_g shown on the right Y axis and T_x and T_p on the left Y axis. With an increase in B_2O_3 content, the glass transition temperature, T_g, and the onset and maximum crystallization temperatures, T_x and T_p, decrease due to more loosely packed structure obtained when SiO_2 is replaced with B_2O_3. The hot forming range, for the second series of glass, is shown in figure 26. Here ΔT presents a maximum of 165 ºC for glass B50. Furthermore, the intensity of the crystallization peak was found to decrease for SiO_2 substitution up to 50% and then increases for higher B_2O_3 content, which may indicate that, in mixed B_2O_3/SiO_2 glass the crystallization is less prone to occur upon heating.

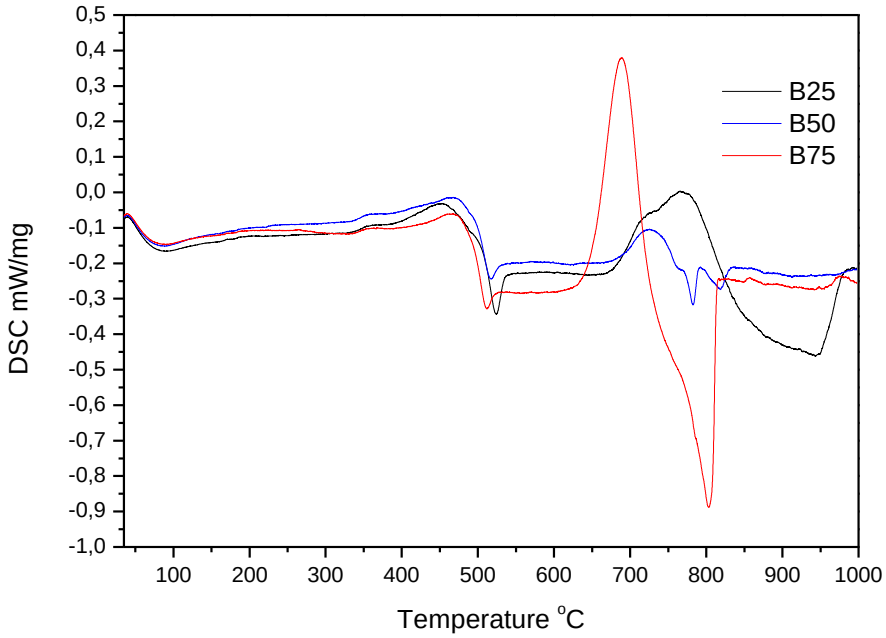

Figure 24: *DTA graph for second series of glass*

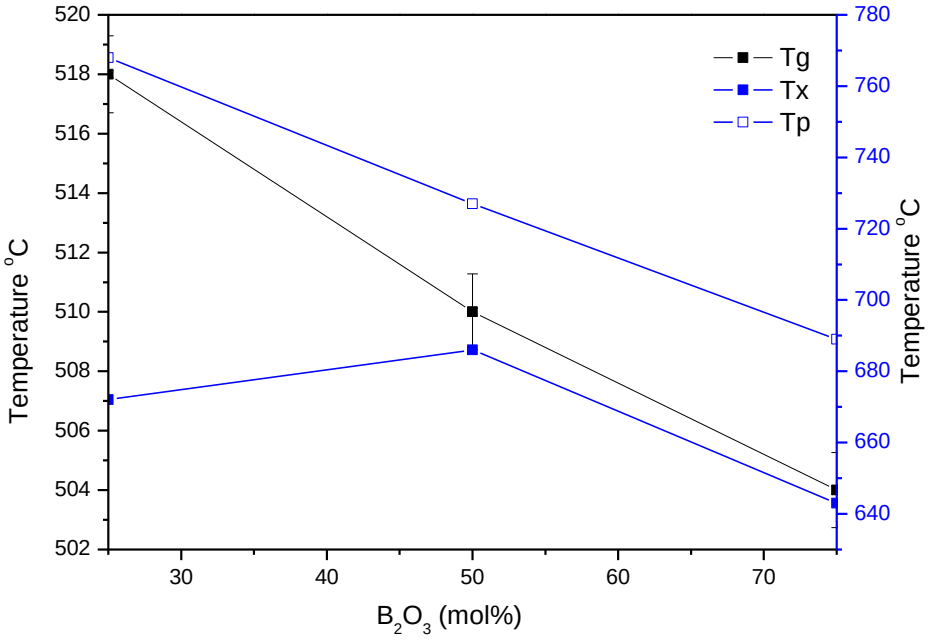

Figure 25: *Tg, Tx and Tp for the second glass series*

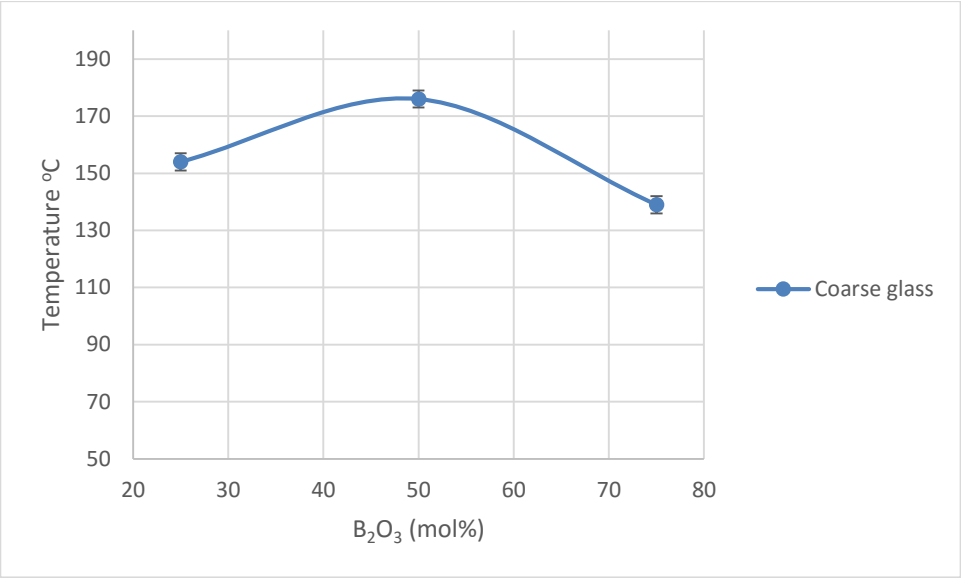

Figure 26: *Hot forming range of second glass series*

4.2.4 *In vitro* dissolution studies

Coarse glass particles were immersed in SBF for 6 to 168 hrs. Figure 27 exhibits the pH of the SBF as a function of immersion time for all glasses of investigation. An increase in B_2O_3 mol% up to 50 % substitution of SiO_2 increases the pH. However, for higher B_2O_3 content, the final pH decreases. As explained earlier, the increase in pH with increasing B_2O_3 content is due to the faster release of alkali and alkaline earth ions from the glass to the solution. The pH for the glass B75 decreases compare to B50 probably due to the higher release of boron. Indeed, boron ions in solution tend to make an acidic by products which should minimize the rise in pH due to the release of Ca and Na. The structural transformation at the surface of the glass' particles, after immersion in SBF, was then studied using FTIR.

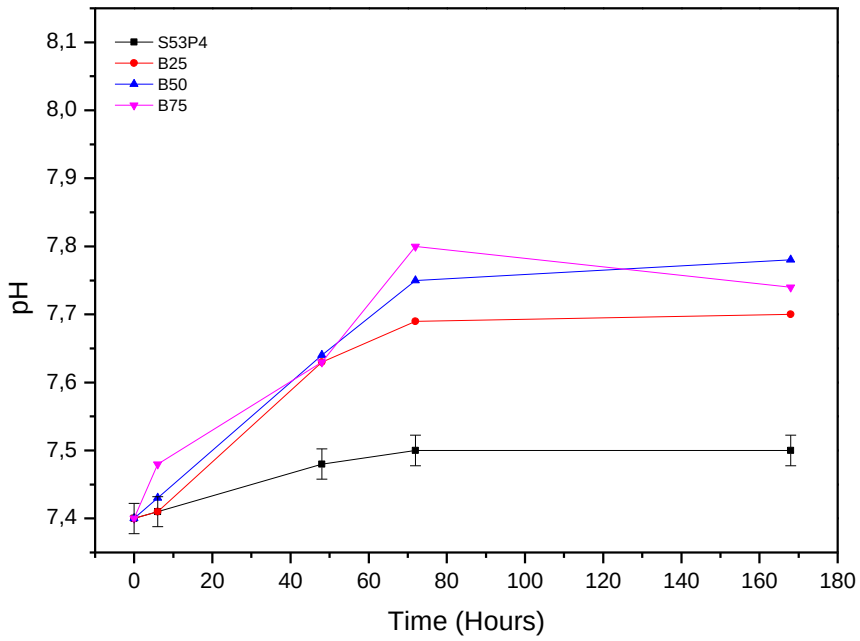

Figure 27: *pH of second series of glass as a function of immersion time. Each point represents mean for two parallel samples.*

The FTIR spectra of the investigated glasses immersed in SBF for various immersion time is given in figure 28, 29 and 30, for the B25, B50 and B75, respectively. When compared to the in vitro FTIR dissolution studies of the first series of glass presented in chapter 4.1, HCA is thicker and more crystallized at the surface of the boron containing glasses with increasing B_2O_3, as seen by the precipitated layer as well as the increase in intensity, with increasing boron content, of the vibration band related to carbonate (Massera *et al.* 2014a). This leads to the conclusion that the second series of glass has more affinity towards the HA formation compared to the first series of glass. The second series of glass converted to HA at earlier immersion time. The second series of glass was hence chosen for the processing of scaffolds, not only because it had good hot forming domain but also a quick and more complete conversion to HA.

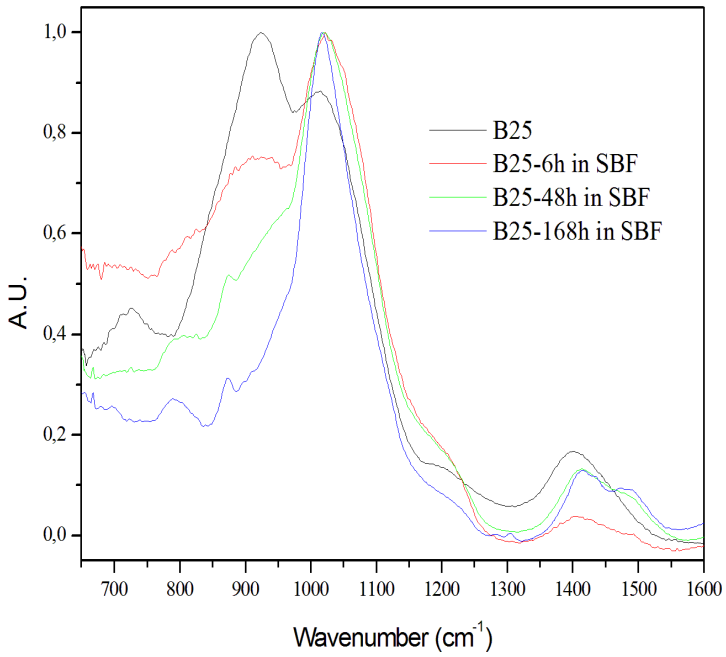

Figure 28: *FTIR spectra B25 glass as a function of immersion time*

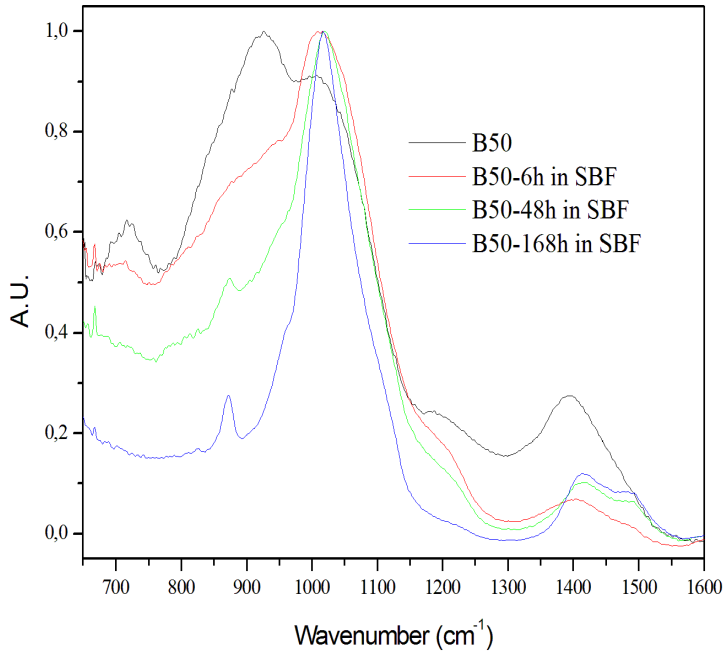

Figure 29: *FTIR spectra B50 glass as a function of immersion time*

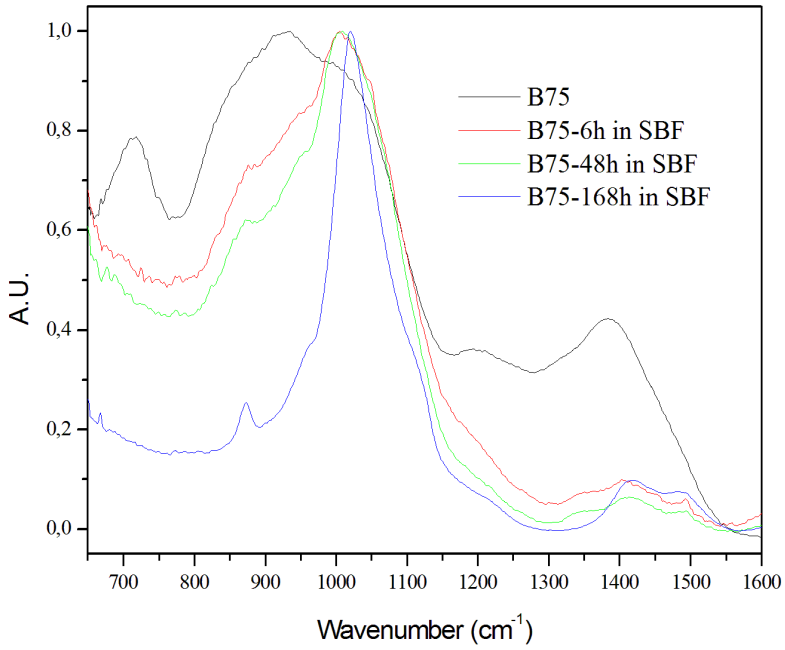

Figure 30: *FTIR spectra B75 glass as a function of immersion time*

4.3 Sintering and scaffold

From the studies of the first and second series of glass, it is clear that the second series have the most promising characteristics for preparing scaffold as they possess large hot forming domain, low crystallization peaks and rapid conversion to HA.

4.3.1 Porosity measurement

Different glass particle sizes (>500 µm, 250-500 µm and <250 µm) were sintered at different temperature (570- 620 ºC). The porosity of the scaffolds is shown in figure 31. The porosities of glass particles increase with an increase in the particle size when using the same sintering temperature. Upon increasing the temperature, the porosity decreases due to the increase in the viscous flow sintering. However, at low temperature the glass particles do not coalesce to form the scaffold. The optimal porosity of around 50% was achieved at 600 ºC for B25 glass, at 580 ºC for B50 glass and at 570 ºC for B75 glass. The scaffolds at the porosity of about 50% did not show any crystallization as checked using XRD.

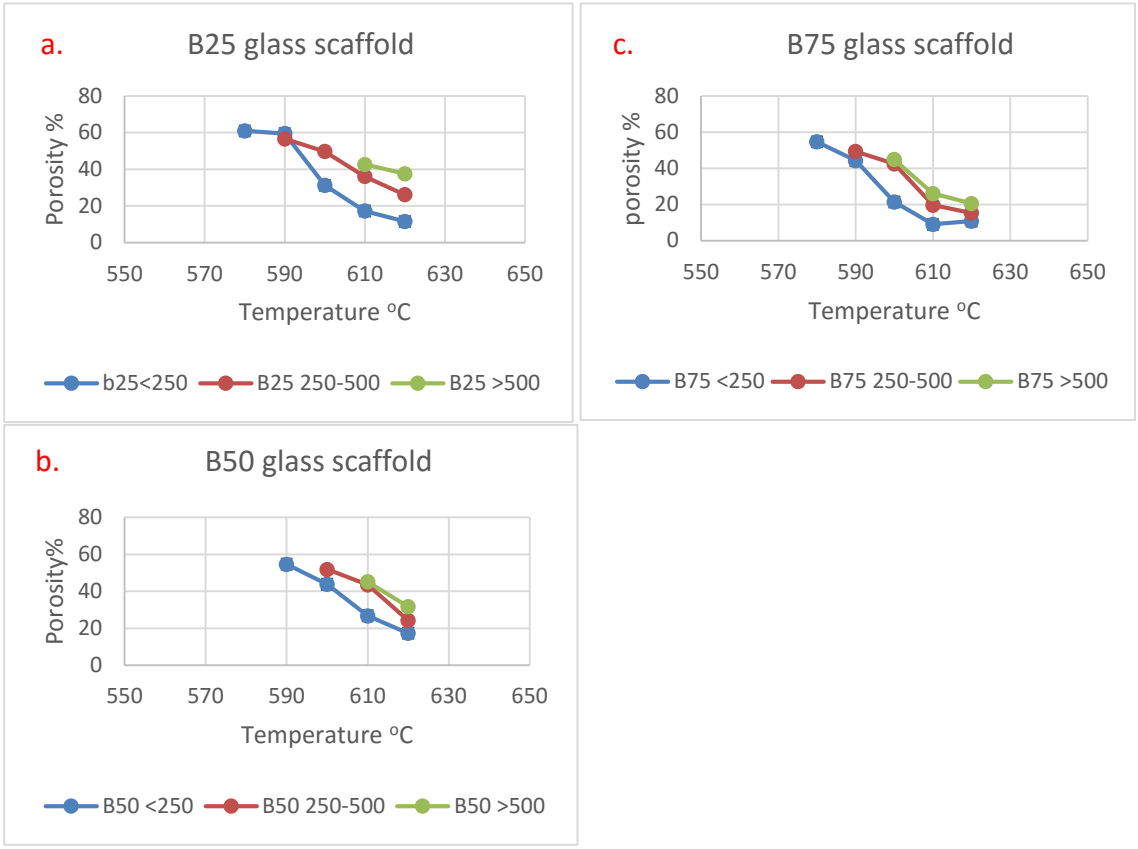

Figure 31: *Porosities of scaffolds at different temperature B25 a) B50 b) and B75 c). Each point represents mean porosities measured in three parallel samples.*

4.3.2 Mechanical strength

The mechanical properties of the glass scaffolds, obtained from sintering of particles in the different particle size, with different porosities were measured as illustrated in fig 32. The mechanical strength decreases drastically for all particle size as the porosity of the scaffold increases. This is due to the increase in void space in the scaffold which makes the scaffold structurally prone to collapse even at lower mechanical stress. Overall 50% porosity was found for the particle size 250-500 µm, which is regarded as an optimum porosity for tissue ingrowth. The compressive strength of the scaffolds with 50% overall porosity was found to range from 3 to 5 MPa, which are close to the one for cancellous bone (Heikkilä 2011).

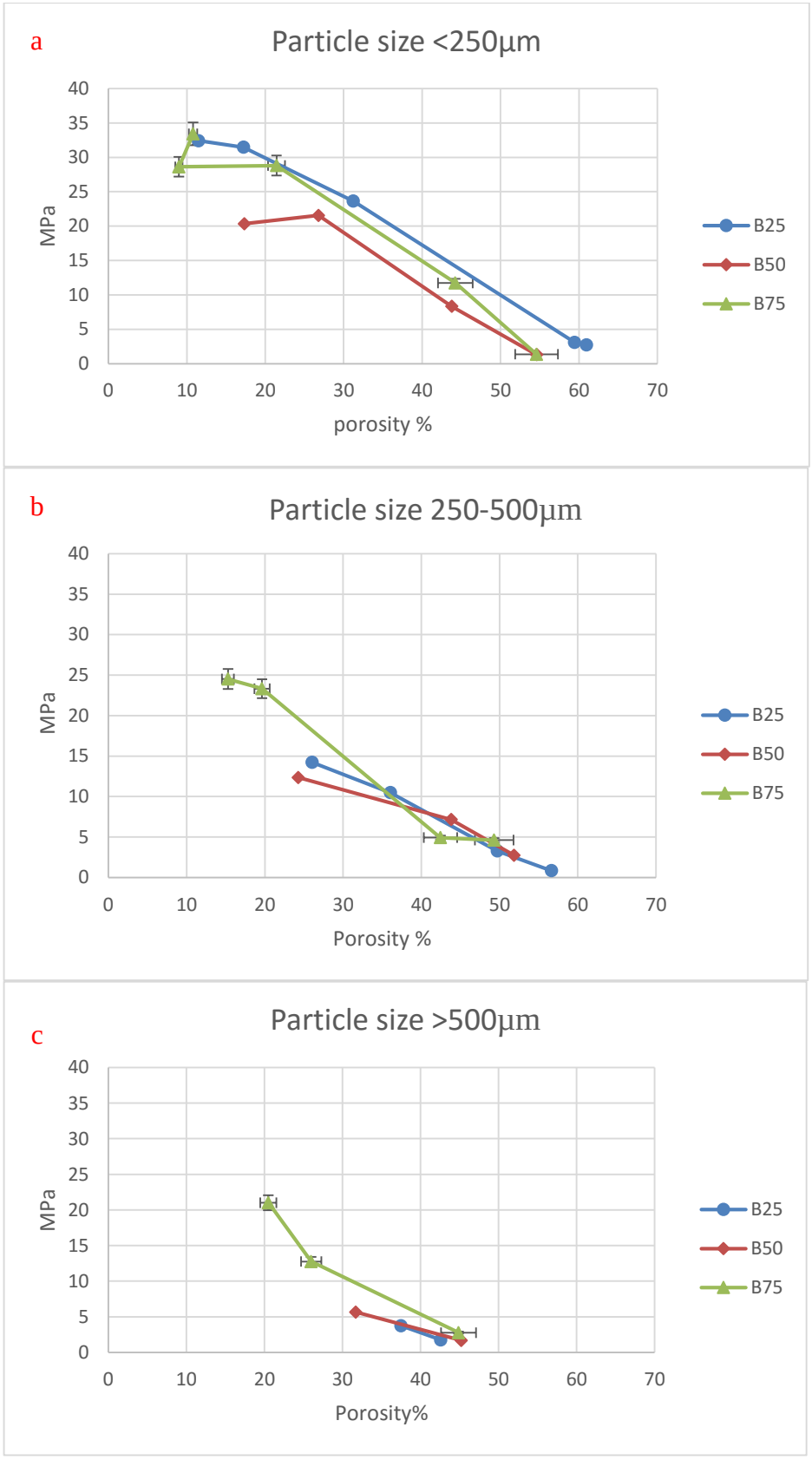

Figure 32: *Compressive strength and porosity <250µm a), 250-500µm b), >500µm c). Each point represents mean for three parallel samples.*

4.3.3 *In vitro* test of scaffold

The sintered scaffolds were immersed in SBF for up to 170h. As shown in figure 33, an increase in pH is seen for all tested samples. The high pH value is due to the high porosity of the materials and thus the high SA in contact with the solution. The pH increase is maximum for the scaffold with composition B50. The lower increase with increasing the boron content to 75% substitution may be due to i) higher B_2O_3 release into the solution or ii) change in the porosity during dissolution of the scaffolds.

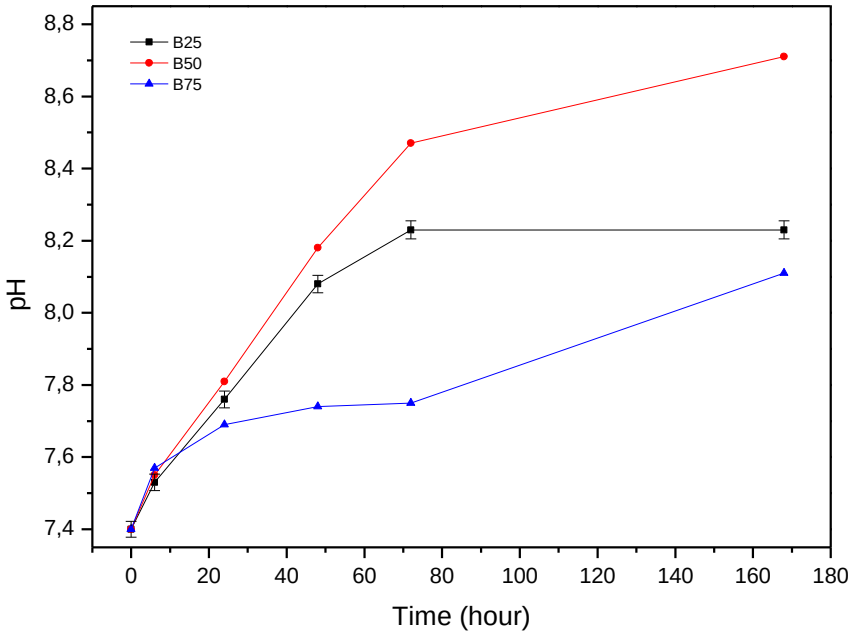

Figure 33: *pH of glass scaffold as a function of immersion time. Each point represents mean for three parallel samples.*

The FTIR spectra of the scaffolds are shown in the figure 34. These spectra are similar to those of the corresponding glasses (see figure 23). The FTIR spectrum of the scaffolds after immersion in SBF are presented in Figures 35 and 36. Already at 6h of immersion, major changes in the main bands within the 900-1200 cm^{-1} range can be seen. This, as expected and explain earlier, is due to the dissolution of the borate and silicate network in the solution. Major changes are seen in scaffold B75 due the faster dissolution of the borate phase compared to the silica phase. However, at one week, the sharp peaks corresponding to the phosphate network vibration in HA are well defined for the scaffolds B25 and B50, whereas no real modification in the structure can be seen for the scaffolds B75 between 6 and 168h of immersion. This indicate that the scaffolds B25 and B50, effectively convert into HA while the dissolution of the scaffolds B75 was slowed down and no significant precipitation of a reactive layer occurred. The reason for such abnormal behavior is not yet fully understood and should be investigated in

more detailed. Indeed, this glass was expected to convert more rapidly and more completely into HA than the two other glass composition. One possible reason could be that the fast dissolution of the glass leads to large amount of debris that prevent the solution form getting in and out of the pores in the scaffolds, thus reducing the SA of the scaffold in contact with the solution.

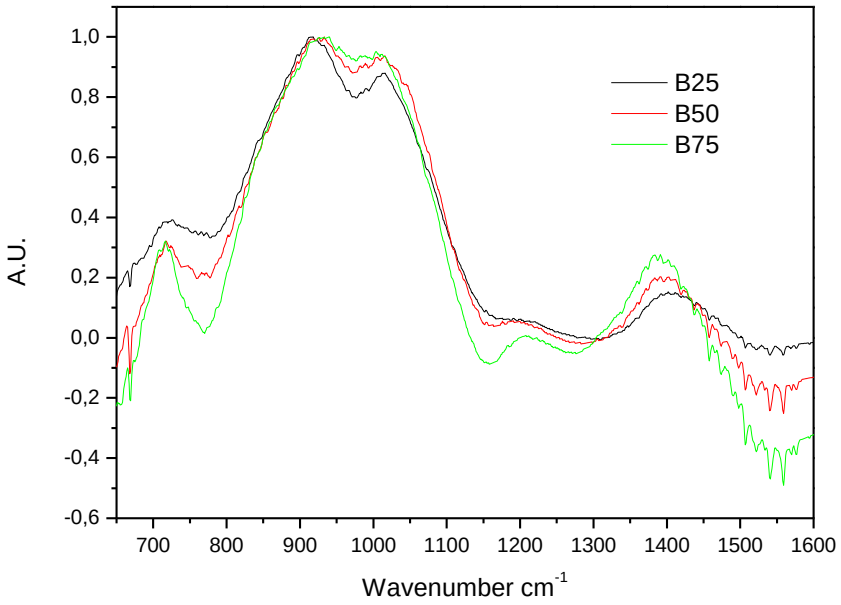

Figure 34: *FTIR of scaffold before immersion in SBF*

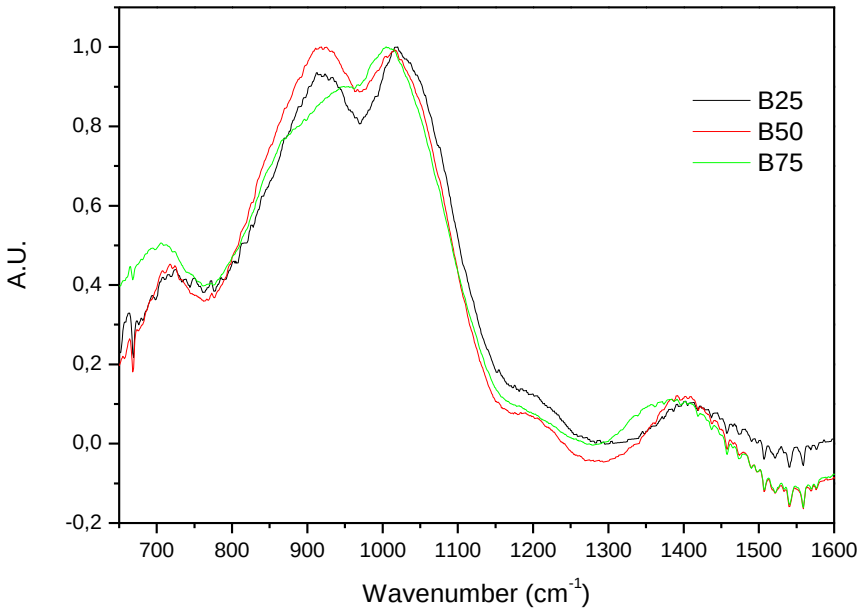

Figure 35: *FTIR of Scaffold immersed 6h in SBF*

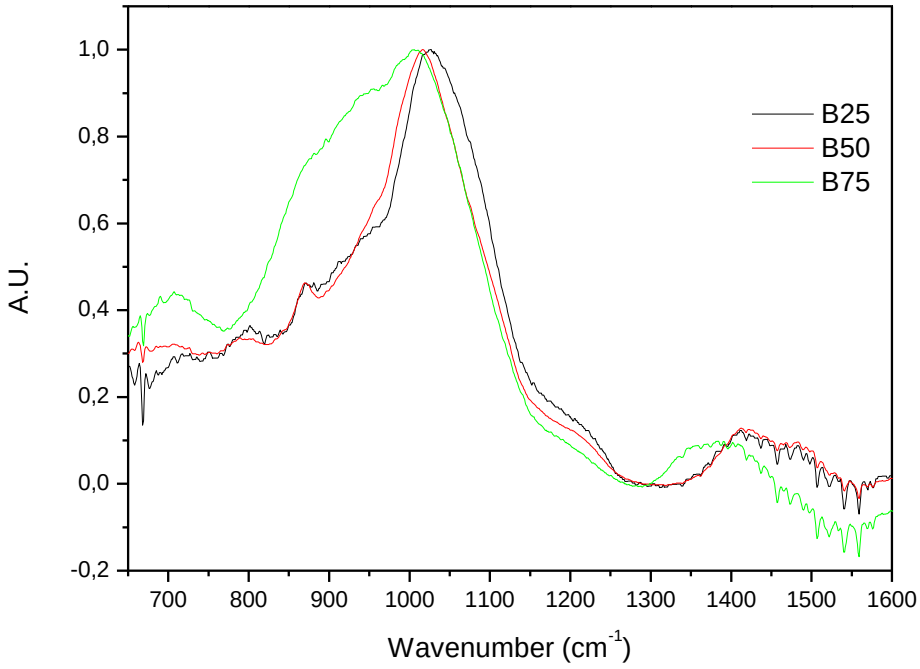

Figure 36: *FTIR of Scaffold immersed 1 week in SBF*

4.3.4 Mechanical properties of scaffold

The compressive strength of the scaffold before and after the immersion in SBF as a function of time is shown in the figure 37. The compressive strength decreases significantly, already after 6 hours of immersion. This early decrease in mechanical strength is due to the pores present in the scaffold which facilitates the leaching of ions from the bulk. This early leaching is also indeed due to the high borate content in the glass scaffold. The glass B25, which is supposed to be the one having the slowest degradation rate was also found to maintain mechanical properties similar to cancellous bone for a longer time. The glass B75 shows a steep decrease in its mechanical properties already at 6 h, similar to the glass B50. This may support our assumption that the glass B75 reacts too fast at short immersion time which leads to drastic compressive strength drop while leading to large amount of debris filling the pores in the scaffolds.

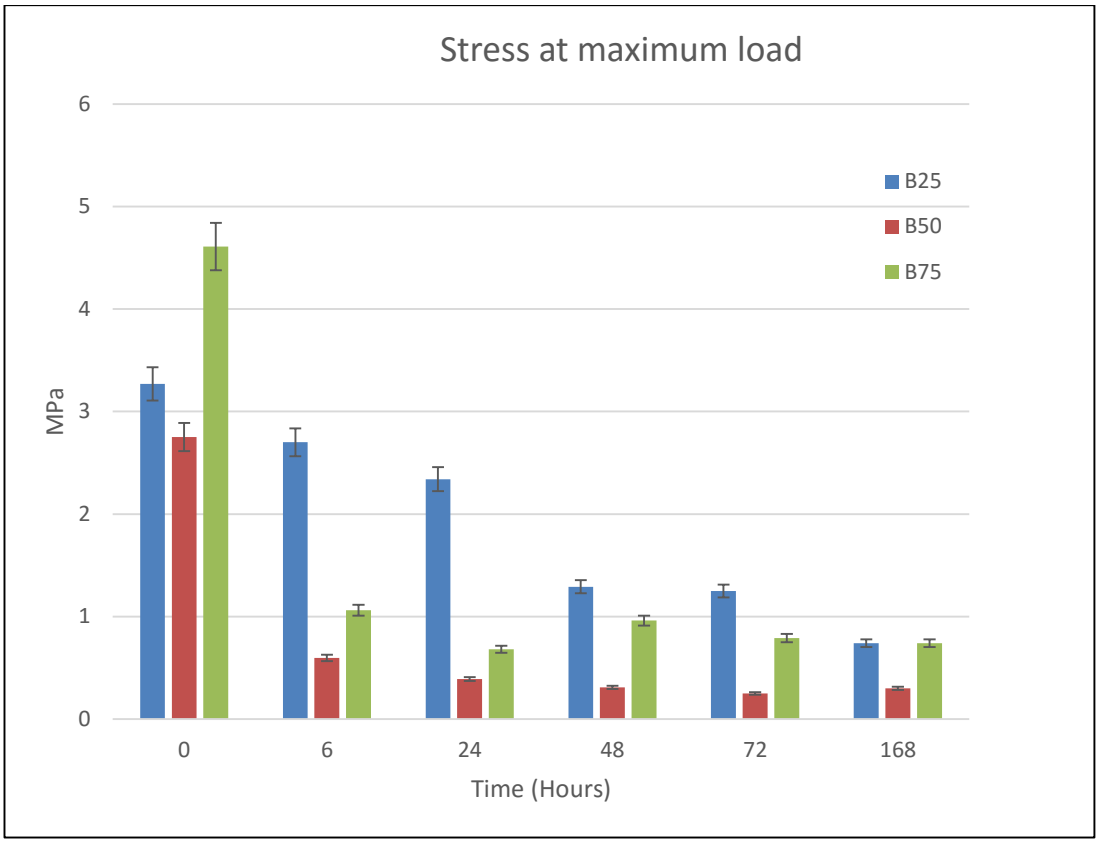

***Figure 37**: Compressive strength of scaffold as a function of immersion time. Each point represents mean for three parallel samples.*

5. CONCLUSION

In this thesis, the impact of boron substitution on silicate glass composition on the thermal and dissolution properties of bioactive glasses was assessed. In general, In TRIS and SBF, addition of boron at the expense of silicate leads to an increase in the dissolution rate and a more rapid formation of HA *in vitro*. The hot forming domain was also found to be enhanced. Only glasses with 25, 50 and 75 % SiO_2 substitution for B_2O_3 exhibited a crystallization peaks indicating a decrease in the crystallization rate.

Scaffolds from these composition (B25, B50 and B75) were processed using simple heat sintering using various temperature and three particles sizes. The use of small particle size led to stronger scaffolds due to a decrease in the average pore size. The use of large pore size, at the opposite, led to a decrease in the compressive strength due to increase in the average pore size (at constant overall porosity). However, it is noteworthy that all scaffolds processed in this thesis maintain their amorphous nature. The scaffold processed with 50% overall porosity using particle size in the range 250 – 500 µm were immersed in SBF. While an increase in boron content led to faster HA formation on glass particles, the same was not seen in the scaffolds. Indeed, the higher B-containing scaffolds was found to degrade rapidly and hence, decrease the mechanical properties.

The borosilicate glass with higher boron content seems to be promising in terms of apatite formation and fabrication of scaffold by sintering. Porosity required for tissue ingrowth has been achieved without losing bioactive properties. Mechanical properties of the scaffold have also been achieved that is comparable to cancellous bone. Overall, this study leads a pathway to the development of borosilicate bioactive glass scaffolds which should be beneficial to tissue-engineering.

REFERENCES

Amini, A.R., Laurencin, C.T. & Nukavarapu, S.P. (2012), Bone Tissue Engineering: Recent Advances and Challenges, Crit Rev Biomed Eng.; 40(5), pp. 363–408.

Andersson, O.H., Karlsson, K.H. & Kangasniemi, K. (1990), Calcium-phosphate formation at the surface of bioactive glass *in vivo*. J. Non-Cryst. Solids; (119), pp. 290–296.

Bellucci, D., Cannillo, V., Ciardelli, G., Gentile, P. & Sola, A. (2010), Potassium based bioactive glass for bone tissue engineering; Ceram. Int., (36), pp.2449–2453.

Bellucci, D., Bolelli, G., Cannillo, V., Cattini, A. & Sola, A. (2011), In situ Raman spectroscopy investigation of bioactive glass reactivity: Simulated body fluid solution vs TRIS-buffered solution, Mater. Charact. 2011; 62(10), pp. 1021-1028.

Bergmann, C.P. & Stumpf, A. (2013), Dental Ceramics, Topics in Mining, Metallurgy and Materials Engineering, Springer; pp. 9-11.

Bi, L., Rahaman, M.N., Day, D., Brown, Z., Samujh, C., Liu, X., Mohammadkhah, A., Dusevich, V., Eick, J.D. & Bonewald, L. (2013), Effect of Bioactive Borate Glass Microstructure on Bone Regeneration, Angiogenesis, and Hydroxyapatite Conversion in a Rat Calvarial Defect Model, Acta Biomater; 9 (8), pp. 8015-8026.

Blaker, J.J., Nazhat, S.N., Boccaccini, A.R. (2004), Development and characterisation of silver-doped bioactive glass-coated sutures for tissue engineering and wound healing applications, Biomaterials; (25), pp. 1319-1329.

Bohner, M. & Lemaitre, J. (2009), Can bioactivity be tested in vitro with SBF solution? , Biomaterials; 30(12), pp. 2175-2179.

Brink, M. (1997), The Influence of Alkali and Alkaline Earths on the Working Range for Bioactive Glasses. J. Biomed Mater. Res.; (36), pp. 109-117.

Bunker, B.C., Arnold, J.A. Wilder, J. (1984), Phosphate glass dissolution in aqueous solutions, Journal of Non-Crystalline Solids, (64) pp. 291–316.

Carter CB, Norton MG. Ceramic Materials Science and engineering, New York: Springer Science+Business media, LLC; 2007.

Chen, G., Ushida,T., & Tateishi,T.(2002), Scaffold Design for Tissue Engineering, Macromol. Biosci.; (2), pp. 67-77.

Chen, Q.Z., hompson, I.D. & Boccaccini, A.R. (2006), 45S5 Bioglass®-derived glass–ceramic scaffolds for bone tissue engineering Biomaterials, (27), pp. 2414–2425.

Clement, J., Manero, J.M., Planell, J.A., Avila, G., Martinez, S. (1999), Analysis of the structural changes of a phosphate glass during its dissolution in simulated body fluid, J Mater Sci Mater Med; (10), pp. 729–732.

Fagerlund, S. (2012), Understanding the *in vitro* dissolution rate of glasses with respect to future clinical applications, Phd thesis, Åbo akademi university; pp. 1-67

Fagerlund, S., Massera, J., Moritz, N. Hupa, L.& Hupa, M. (2012a), Phase composition and in vitro bioactivity of porous implants made of bioactive glass S53P4, Acta Biomaterialia; 8(6), pp. 2331-2339.

Fagerlund, S., Massera, J., Hupa, M., & Hupa, L. (2012b), T–T–T behaviour of bioactive glasses 1–98 and 13–93, Journal of the European Ceramic Society;(32), pp. 2731–2738.

Fagerlund, S., Hupa, M., & Hupa, L. (2013), Dissolution patterns of biocompatible glasses in 2-amino-2-hydroxymethyl-propane-1,3-diol (Tris) buffer; Acta Biomaterialia, 9(2) 2013, pp. 5400-5410.

Fu, Q., Rahman, M.N., Fu, H. & Liu, X. (2010), Silicate, borosilicate, and borate bioactive glass scaffolds with controllable degradation rate for bone tissue engineering applications. I. Preparation and *in vitro* degradation, journal of biomedical materials research part A; 95A (1), pp.164-171.

George, J.L., "Dissolution of borate glasses and precipitation of phosphate compounds" (2015). Doctoral Dissertations, Missouri University of Science and Technology, USA, Paper 2382.

Georgiou, G., Mathieu, L., Pioletti, D. P., Bourban, P.-E., Månson, J.-A. E., Knowles, J. C.& Nazhat, S. N. (2007), Polylactic acid–phosphate glass composite foams as scaffolds for bone tissue engineering. J. Biomed. Mater. Res., 80B: 322–331

Gerhardt, L.C. & Boccaccini, A.R. (2010), Bioactive Glass and Glass-Ceramic Scaffolds for Bone Tissue Engineering, Materials; (3), pp. 3867-3910.

Hanna, A. (2008), Crystallization characteristics of bioactive glass, Phd thesis, Åbo akademi university; pp. 1-49.

Heikkilä, J. (2011), Use of bioactive glasses as bone substitutes in orthopaedics and traumatology. In Bioactive Glasses Materials, properties and applications ed. H. Ylänen. Woodhead publishing in Materials, Cambridge, pp. 189-208.

Hench, L.L., Splinter, R.J., Allen, W.C. & Greenlee TK Jr., (1972), Bonding mechanisms at the interface of ceramic prosthetic materials, Journal of Biomedical Material Research, (2), pp. 117-141.

Hench, L. L., Andersson, Ö. H. & LaTorre, G. P. (1991), Surface reactions of bioactive glasses compared with an inactive glass, The kinetics of bioactive ceramics part III: Bioceramics 4, ed. Bonfield, W., Hastings, G.W. & Tanner, W., Pergamon/Elsevier, Oxford; pp. 156-162.

Hench, L.L. (1991), Bioceramics: From Concept to Clinic, Journal of American Ceramic Society; (7), pp. 1487–1510.

Hench, L. L. & Latorre, G. P. (1992), Effect of glass and solution composition, Reaction kinetics of bioactive ceramics; (4), pp. 767-774.

Hench, L.L. (1998), Bioceramics, Journal of American Ceramic Society; (81), pp. 1705-1728.

Hench, L.L. (2006), The story of Bioglass, J Mater Sci: Mater Med, (17), pp.967–978.

Huang, W., Day, D.E., Kittiratanapiboon, K. & Rahaman, M.N. (2006), Kinetics and mechanisms of the conversion of silicate (45S5), borate, and borosilicate glasses to hydroxyapatite in dilute phosphate solutions, J Mater Sci Mater Med.; 17(7), pp. 583-596.

Jones, J.R. & Hench, L.L. (2003), Regeneration of trabecular bone using porous ceramics. Curr Opin Solid State Mater Sci.; (7), pp 301-307.

Jones, J.R., Ehrenfied L.M. & Hench, L.L. (2006), Optimising bioactive glass scaffolds for bone tissue engineering, Biomaterials; 27(7), pp. 964-973.

Kokubo, T., Kushitani, H., Sakka, S., Kitsugi, T. & Yamamuro, T. (1990), Solutions able to reproduce *in vivo* surface-structure changes in bioactive glass-ceramic A-W^3, J. Biomed. Mater. Res.; (24), pp.721–734.

Kokubo, T. (1991), Bioactive glass ceramics: properties and applications, Biomaterials; (12): 155–163.

Kokubo, T & Takadama, H. (2006), How useful is SBF in predicting *in vivo* bone bioactivity? Biomaterials; 27(15), pp. 2907-2915.

Liang, W., Rüssel, C., Day, D.E., & Völksch, G. (2006), Bioactive comparison of a borate, phosphate and silicate glass. Journal of Materials Research; (21), pp. 125-131.

Lindfors, N.C. (2011), Clinical Experience on Bioactive Glass S53P4 in Reconstructive Surgery in the Upper Extremity Showing Bone Remodelling, Vascularization, Cartilage Repair and Antibacterial Properties of S53P4; Journal of Biotechnology and Biomaterials, (1), pp. 1-5.

Lu, H. H., El-Amin, S. F., Scott, K. D.& Laurencin, C. T. (2003), Three-dimensional, bioactive, biodegradable, polymer–bioactive glass composite scaffolds with improved mechanical properties support collagen synthesis and mineralization of human osteoblast-like cells in vitro, J. Biomed. Mater. Res. A;(64), pp. 465–474.

Massera, J., Fagerlund, S., Hupa, L. & Hupa, M. (2012), Crystallization Mechanism of the Bioactive Glasses, 45S5 and S53P4. J. Am. Ceram. Soc., (95), pp. 607–613.

Massera, J & Hupa, M. (2014a), Influence of SrO substitution for CaO on the properties of bioactive glass S53P4, J Mater Sci: Mater Med; (25), pp. 657–668.

Massera, J., Ahmed, I., Petit, L., Aallos, V. & Hupa, L. (2014b), Phosphate-based glass fiber vs. bulk glass: Change in fiber optical response to probe in vitro glass reactivity, (37), pp. 251-257.

Massera, J., Mayran, M., Rocherullè, J, & Hupa, L (2015), Crystallization behavior of phosphate glasses and its impact on the glasses' bioactivity, Journal of material science, 50(8), pp. 3091-3102.

Nayak, J.P., Kumar, S. & Bera, J. (2010), Sol-Gel Synthesis of Bioglass-Ceramics Using Rice Husk Ash as a Source for Silica and Its Characterization, Journal of Non-Crystalline Solids; (365), pp. 1447-1451.

Ning, J., Yao, A., Wang, D., Huang, W., Fu, H., Liu, X., Jiang, X., & Zhang, X. (2007), Synthesis and *in vitro* bioactivity of a borate-based bioglass, Material Letters, 61(30), pp. 5223-5226.

Padmaja G. & Kistaiah P. (2009), Infrared and Raman spectroscopic studies on Alkali Borate glasses: Evidence of mixed alkali effect, Journal of physical chemistry: A;(113), pp. 2397-2404.

Pascuta, P., Bosca, M., Rada, S., Culea, M. & Bratu, I. (2008), FTIR Spectroscopic Study of Gd2O3-Bi2O3-B2O3 Glasses, Journal of Optoelectronics and Advanced Materials; (10), pp. 2416-2419.

Peltola, M. J. & Aitasalo, K. M. J. (2011), Bioactive glass for maxillofacial and dental repair, Bioactive glasses Materials, properties, applications, ed. H. Ylänen. Woodhead publishing in Materials, Cambridge; pp. 217-226.

Queiroz, A.C., Santos, J.D., Monteiro, F.J. & Prado da Silva, M.H. (2003), Dissolution Studies of Hydroxyapatite and Glass-Ceramic Reinforced Ceramics, Materials Characterization; (50) pp. 197-202.

Rahaman, M.N., Delbert, E.D., Bal, S., Fu, Q., Jung, S.B., Bonewald, L.P. & Tomsia A.P. (2011), Review: Bioactive glass in tissue engineering, Acta Biomaterialia; (7), pp. 2355–2373.

Rahaman, M.N., Bal, S. & Huang, W. (2014), Review: Emerging developments in the use of bioactive glasses for treating infected prosthetic joints, Materials Science and Engineering C; (41), pp. 224–231.

Ristić, M.M. & Milosevic, S.D. (2006), Frenkel's Theory of Sintering, Science of Sintering; (38), pp. 7-11.

Rohanová, D., Boccaccini, A.R., Yunos, D.M., Horkavcová, D., Březovská, I. & Helebrant, A. (2011), TRIS buffer in simulated body fluid distorts the assessment of glass–ceramic scaffold bioactivity. Acta Biomaterialia; 7(6), pp. 2623-2630.

Serra, J., González, P., Liste, S., Serra, C., Chiussi, S., León, B., Pérez-Amor, M., Ylänen, H.O. & Hupa, M. (2003), FTIR and XPS Studies of Bioactive Silica Based Glasses, Journal of Non-Crystalline Solids; (332), pp. 20-27.

Tsuruga, E., Takita, H., Itoh, H., Wakisaka, Y. & Kuboki, Y. (1997), Pore size of porous hydroxyapatite as the cell-substratum controls BMP-induced osteogenesis, J Biochem (Tokyo); 121(2), pp. 317–324.

Varila, L., Fagerlund,S., Hupa,L., Lehtonen,T. and Tuominen,J. (2012), Surface reactions of bioactive glasses in buffered solution, Journal of the European Ceramic Society (32), pp. 2757–2763.

Varshneya A, K. Fundamentals of Inorganic Glasses, Sheffield: The Society of Glass Technology; 2006.

Vedel, E., Arstila, H., Zhang, D., Hupa, L. & Hupa, M. (2007), Control of the forming properties of bioactive glasses, Proc. Eighth Eur. Soc. Glass Sci Technol. Conf. Glass Technol.: Eur. J. Glass Sci. Technol. A, 48 (4)
Wallenberger, F.T. & Smrcek, A. (2010), The Liquidus Temperature; Its Critical Role in Glass Manufacturing. Int. J. Appl. Glass Sci. 2010; 1(2), pp. 151-63.

Williams, D.F. (2009), On the nature of biomaterials, Biomaterials; (30), pp. 5897-5909.

Xynos, I.D., Edgar, A.J., Buttery, L.D.K., Hench, L.L. & Polak, M. (2001), Gene expression profiling of human osteoblasts following treatment with the ionic products of

Bioglass® 45S5 dissolution, Journal of Biomedical Material Research; (55), pp. 151-157.

Yao, A., Wang, D., Huang, W., Fu, Q., Rahaman, M. N. & Day, D. E. (2007), *In Vitro* Bioactive Characteristics of Borate-Based Glasses with Controllable Degradation Behavior, Journal of the American Ceramic Society; (90), pp. 303–306.

Ylänen. H, Karlsson, K.H., Itälä, A.& Aro, H.T. (2000), Effect of immersion in SBF on porous bioactive bodies made by sintering bioactive glass microspheres. J. Non Cryst. Solids; (275), pp. 107-15.

Zhang, X., Jia, W., Gu, Y., Liu, X., Wang, D., & Zhang, C. (2010), Teicoplanin-loaded borate bioactive glass implants for treating chronic bone infection in a rabbit tibia osteomyelitis model, Biomaterials; (31), pp. 5865–5874.